Progress Report

IDENTIFICATION AND LOCATION OF DAMAGES IN STRUCTURES BY THE SYSTEM IDENTIFICATION TECHNIQUE

by

Department of Mechanical Engineering
The University of Maryland
College Park, Maryland 20742

Principal Investigator: Jackson C. S. Yang
Professor

May 18, 1984

TABLE OF CONTENTS

List of Tables ii

List of Figures iii

1. Summary 1

2. Introduction 2

3. Objectives 4

4. Approach 5

4.1 Math Model 5

4.2 System Identification Techniques 9

4.2.1 Frequency Domain Technique

4.2.2 Time Domain Technique

4.3 Computer Program Development 12

4.4 Performance Test of the Time Domain Algorithm 13

4.5 Performance Test of the Frequency Domain Algorithm 16

4.6 Performance Test of the System Identification Algorithm

5. Analog Computer Experiment 17

6. Cantilever Beam Experiment 40

7. NASTRAN Simulation 40

8. Conclusion/Recommendation 56

Appendix I Random Decrement Analysis Identification Algorithm 58

Appendix II Frequency Domain Curve Fitting Method 63

References 76

List of Tables

Tables		Page
1.	Theoretical test cases of the time domain program	14
2.	Poles and residues of the velocity transfer functions (1st stage damage	22
3.	Poles and residues of the velocity transfer functions (2nd stage damage)	27
4.	Poles and residues of the velocity transfer functions (3rd stage damage)	27
5.	Frequencies, dampings and amplitudes of the time responses (1st stage damage)	36
6.	Frequencies, dampings and amplitudes of the time responses (2nd stage damage)	37
7.	Frequencies, dampings and amplitudes of the time responses (3rd stage damage)	38
8.	Normalized damping and stiffness matrices	39
9.	Natural frequencies of the beam calculated by NASTRAN	48
10.	Added modal damping ratios	48
II-1.	Exact System Coefficients	68
II-2.	Identified System Coefficients - New Algorithm	68
II-3.	Identified System Coefficients - Sanathanan and Koerner Algorithm	69

List of Figures

Figures		Page
1.	Overall program approach	6
2.	System identification technique	10
3.	Two-degrees-of-freedom system with well-separated modes	18
4.	Two-degrees-of-freedom system with closely-spaced modes	19
5.	Three-degrees-of-freedom system	20
6.	Analog computer setup	21
7.	Velocity transfer function of mass 1 with force applied at mass 2	23
8.	Velocity transfer function of mass 2 with force applied at mass 2	24
9.	Velocity time response at mass 1, with constant force at mass 2	30
10.	Velocity time response at mass 2, with constant force at mass 2	31
11.	Displacement time response at mass 1, with constant force at mass 2	32
12.	Displacement time response at mass 2, with constant force at mass 2	33
13.	Displacement time response at mass 1, with constant force at mass 1	34
14.	Displacement time response at mass 2, with constant force at mass 1	35
15.	The cantilever beam system	41
16.	Transfer functions at location 1, with force at location 5	42
17.	Transfer functions at location 2, with force at location 5	43
18.	Transfer functions at location 3, with force at location 5	44
19.	Transfer functions at location 4, with force at location 5	45
20.	Transfer functions at location 5, with force at location 5.	46

21.	Transfer functions at location 6, with force at location 6	47
22.	Finite element mesh configuration used in the NASTRAN simulation	49
23.	Simulated transfer function at location 1, with force at location 5 (no crack)	50
24.	Simulated transfer function at location 2, with force at location 5 (no crack)	51
25.	Simulated transfer function at location 3, with force at location 5 (no crack)	52
26.	Simulated transfer function at location 4, with force at location 5 (no crack)	53
27.	Simulated transfer function at location 5, with force at location 5 (no crack)	54
28.	Simulated transfer function at location 6, with force at location 5 (no crack)	55
I-1.	Principles of Randomdec Technique	60
I-2.	Extraction of the Randomdec signature	61
II-1.	Frequency response, real and imaginary	70
II-2.	Frequency response, magnitude and phase angle	71
II-3.	Fitted frequency response, real and imaginary, with new algorithm	72
II-4.	Fitted frequency response, magnitude and phase angle, with new algorithm	73
II-5.	Fitted frequency response, real and imaginary, with Sanathanan and Koerner algorithm	74
II-6.	Fitted frequency response, magnitude and phase angle, with Sanathanan and Koerner algorithm	75

1. Summary

Complex systems such as naval ship structures and offshore platforms are exposed to severe loadings which over an extended time period can cause damage in the form of fractures and cracks which can ultimately lead to fatigue failures. The work conducted under this research involved the development of a System Identification technique which has the potential of detecting and tracking progressive fracture by observed changes in the identified system parameters; namely the mass [M], damping [C], and stiffness [K] matrices. Although cracks have long been known to cause changes in resonant frequencies, changes in the [M][C][K] matrices appear to be more significant and hence more detectable. In addition, one might relate the changes in the matrices to changes in the actual physical system. Mathematical theory was developed which, when implemented in a computer algorithm, allows the eigenvalues and eigenvectors to be extracted from the structural response for a known random type forcing function. Knowing the eigenvalues and eigenvectors, the [M][C][K] matrices can be accurately determined.

Analog computer studies simulating discrete spring-mass-dashpot systems demonstrated that the identified system parameters can be retrieved quite accurately from response data. Laboratory experiments on a cantilever beam with induced saw cuts to simulate a propagating crack demonstrated that the effect of crack depth is manifested in observed changes to the [M][C][K] matrices as well as changes to the power spectral density and resonant frequencies. Finite element structural analysis of the cantilever beam also showed detectable changes in the resonant frequencies; particularly at the higher modes.

A logical extension of this research is proposed to correlate damage with changes in the identified system parameters.

2. Introduction

Many ship and offshore structures have a predicted design life which is generally based on conservative design criteria to compensate for uncertainties in the load environment and associated damage effects. For example, complex systems such as naval ship structures and offshore platforms are exposed to severe wave loading which over an extended period can lead to fatigue failures. Initiation and propagation of cracks change the structural response of the system which manifests itself in a change in the dynamic equations of motion. The System Identification technique, whereby the dynamic equations of motion can be deduced from experimental data, offers the potential of being able to detect cracks, flaws, etc. by observed changes in the Identified System Parameters such as stiffness, mass and damping matrices.

Random decrement system identification and defect correlation analysis of structural systems offer the prospect of reliably tracking progressive pre-catastrophic type damage. It would establish a technology base of truly being able to only retire flight vehicles for cause rather than their reaching a certain number of flight vehicle hours of use.

The identification and modeling of multi-degree of freedom dynamic systems through the use of experimental data is a problem of considerable importance in the area of system dynamics, automatic controls and structural analysis (1-21). Indicative of the wide range of applicability of this subject is a recent survey article (4) which contains over 130 references related to system and parameter identification.

This mathematical model representation may prove to be a very powerful tool for the analysis and design of complex systems. The mathematical model

representation could of course be derived from the theoretical knowledge of the system and its components, or from a finite elements model in the case of purely structural systems. These techniques though are inferior compared to one which is based on actual experimental response data. Furthermore as the systems become more complex and sophisticated it is becoming more and more difficult to understand their behavior to develop theoretical models to predict their response.

3. Objectives of Study

The objective is to develop new and more accurate dynamic system identification techniques to determine the dyanmic equations of motion from dynamic response data for systems with high modal density. It is desired to demonstrate that it is feasible to detect damage in structures from cracks/flaws by observed changes in the Identified System Parameters such as the mass [M], stiffness [K] and damping [C] matrices as well as to changes in the power spectral density and resonant frequencies. The ultimate objective of subsequent research is to correlate the crack/flaw size and location with observed changes in the System Parameter.

4. Approach

The basic approach used to identify changes in the System Parameters from damage to the structure is illustrated in Figure 1. First the mathematical theory is developed which essentially involves developing the equations of motion in a form which allows the eigenvalues, eigenvectors, mass matrix [M], stiffness matrix [K], and damping matrices [C] to be determined from measured response data. Computer programs were developed to facilitate this using the time domain technique and frequency domain technique (both techniques are described in this section) to retrieve the eigenvalues, eigenvectors from the response data, and then use those to compute the mass [M], stiffness [K] and damping [C] matrices. A systematic procedure was used to test the algorithms to ensure that the eigenvalues, eigenvectors could be accurately retrieved from the response data by an improved curve fitting and autoregressive techniques developed by the University of Maryland. Analog computer studies were then conducted to demonstrate the ability of the computer program to retrieve the system parameters from response data of simulated structures involving spring, mass, dashpot systems. These studies were also designed to demonstrate that simulated damage can be detected by changes in the System Parameters. Finally, experimental tests and theoretical finite element analyses were conducted of a cantilever beam to demonstrate that crack size does exhibit changes in the Identified System Parameters which are detectable. Detailed description of all these tasks are included in the following.

4.1 Mathematical Model of the System Identification Technique

Consider a structural system which can generally be represented by an N

Figure 1

Overall Program Approach

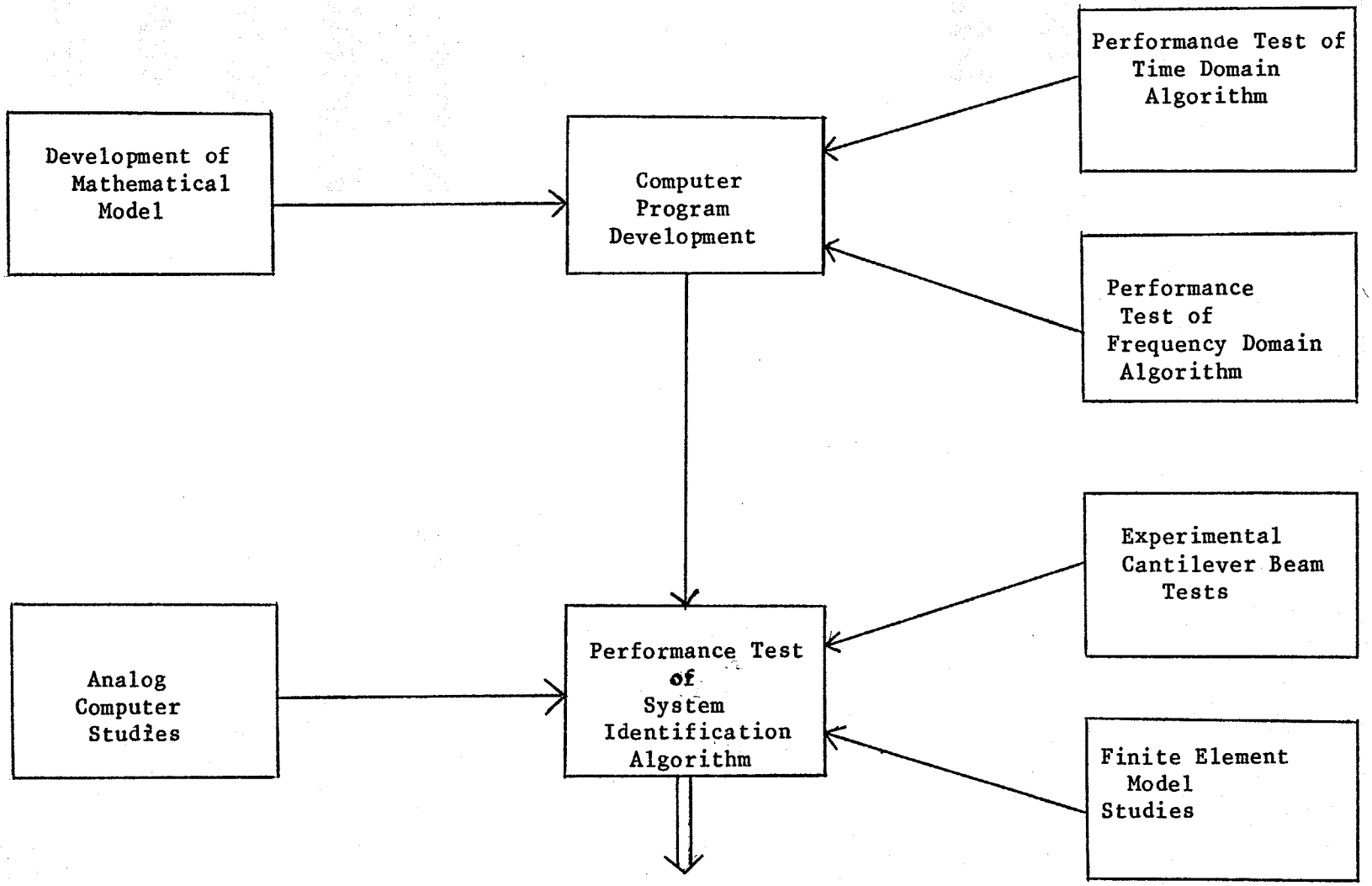

Feasibility of detecting 'Simulated Damage from Changes in System Identification' Parameters

degree-of-freedom linear system. The dynamics of the system is governed by its equation of motion

$$[\,M\,][\,\ddot{X}\,] + [\,C\,][\,\dot{X}\,] + [\,K\,][\,X\,] = [\,f\,],$$

where $[X]$, $[\dot{X}]$, $[\ddot{X}]$ are the displacement, velocity and acceleration column vector of degree N, respectively. $[f]$ is the force column of degree N. $[M]$, $[C]$, $[K]$ are the NxN mass, damping and stiffness matrices, respectively. The exercise of the system identification involves the identification of $[M]$, $[C]$, $[K]$ matrices from the known responses $[\ddot{X}]$, $[\dot{X}]$, $[X]$, and the known forcing function $[f]$.

Adding a trivial differential equation

$$[\,M\,][\,\dot{X}\,] - [\,M\,][\,\dot{X}\,] = 0$$

to the above dynamic equation, we obtain a set of state equations which still describe the motion of the structural system,

$$\left[\begin{array}{c|c} [\,0\,] & [\,M\,] \\ \hline [\,M\,] & [\,C\,] \end{array}\right] \left\{\begin{array}{c} \ddot{X} \\ \hline \dot{X} \end{array}\right\} + \left[\begin{array}{c|c} -[\,M\,] & [\,0\,] \\ \hline [\,0\,] & [\,K\,] \end{array}\right] \left\{\begin{array}{c} \dot{X} \\ \hline X \end{array}\right\} = \left\{\begin{array}{c} 0 \\ \hline f \end{array}\right\}$$

or

$$[\,D\,][\,\dot{q}\,] + [\,E\,][\,q\,] = [\,Q\,],$$

where

$$[D] = \left[\begin{array}{c|c} [0] & [M] \\ \hline [M] & [C] \end{array}\right]$$

$$[E] = \left[\begin{array}{c|c} -[M] & [0] \\ \hline [0] & [K] \end{array}\right]$$

$$[\dot{q}] = \left[\begin{array}{c} \ddot{X} \\ \hline \dot{X} \end{array}\right], \quad [q] = \left[\begin{array}{c} \dot{X} \\ \hline X \end{array}\right], \quad [Q] = \left[\begin{array}{c} 0 \\ \hline f \end{array}\right].$$

After Laplace transformation, we obtain

$$[B(s)][q(s)] = [Q(s)],$$

where $[B(s)] = [[D]s + [E]]$ is the system matrix.

It can be proved that [D] and [E] can be represented by the eigenvalues, P_k, and eigenvectors, $[Y_k]$, of the system matrix which are determined by the homogeneous equation

$$[B(P_k)][y_k] = 0$$

When [M], [C], [K] are all symmetric, the expressions are

$$[D] = [Y]^{-1T}[I][Y]^{-1}$$

$$[E] = [Y]^{-1T}[-P][Y]^{-1}$$

where $Y = [y_1, y_2, y_3, \ldots\ldots, y_N]$ is the eigenvector matrix,

$$P = \begin{bmatrix} P_1 & & & 0 \\ & P_2 & & \\ & & \ddots & \\ 0 & & & P_n \end{bmatrix}$$ is the eigenvalue matrix.

it can also be shown that the system's transfer function can be represented by the eigenvectors and eigenvalues,

$$[H(s)] = [Y](s-P)^{-1}[Y]^T = \sum_{k=1}^{N}\left[\frac{y_k y_k^T}{s-p_k} + \frac{y_k^* y_k^{*T}}{s-p_k^*}\right].$$

The above derivation states the fact that if one can determine the eigenvalues and eigenvectors of a system, the mass, stiffness and damping matrices of the system are simply the products of the eigenvalue and eigenvector matrices. The eigenvalues and eigenvectors can be obtained from the measured system response data for a known force input using frequency domain technique or a time domain technique.

4.2 System Identification Technique

Implementation of the Mathematical Model in the System Identification Technique is illustrated in Figure 2. The random vibrational response of a structural system contains the characteristic signal of the structure. Using proper signal processing techniques, the characteristic signal can be retrieved from the random response. Structural damages can then be identified by studying the changes of the characteristics signal.

Two signal processing techniques have been developed to retrieve the structural characteristic signal from the random responses. One technique analyzes the structure signal in the frequency domain, the other in the time domain.

4.2.1 Frequency Domain Technique

Structural responses from a known random force input are collected into a Fast Fourier Transform (FFT) analyzer to obtain the frequency response in digital form. The digitized frequency responses are curve fitted with a computer program to yield the eigenvalues and eigenvectors. The frequency

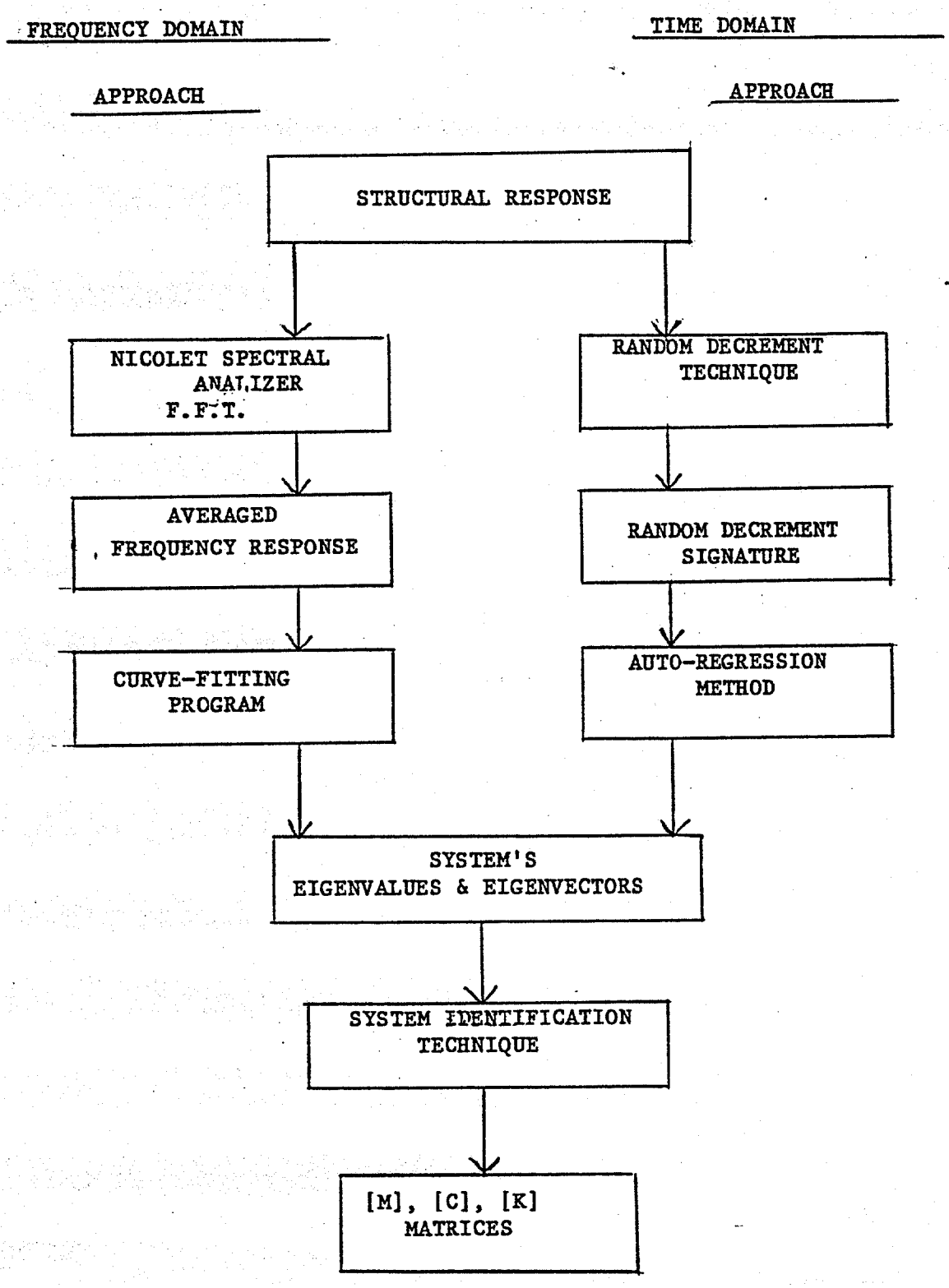

FIGURE 2 SYSTEM IDENTIFICATION TECHNIQUE

domain curve fitting program uses a linear-least square method to find the best fit of the collected system's transfer function to the following theoretical expression

$$H(s) = \sum_{k=1}^{N} \left(\frac{a_k}{s-p_k} + \frac{a_k^*}{s-p_k} \right)$$

where p_k and a_k are the poles and residues of the transfer function. The poles are the system's eigenvalues and the residues related to the eigenvectors. After the eigenvalues and eigenvectors are found, the system identification techniques are applied to find the mass, stiffness and damping matrices. This is described later in the report.

4.2.2 Time Domain Technique

The time responses of a structure system when excited by a random forcing function is digitized and processed with random decrement technique. The random decrement signature represents system's characteristics from which the system's modal frequencies and damping values can be determined. The details of the random decrement technique are described in Appendix I.

The impulse response of a structure system contains the characteristic time function of the system. The frequencies and damping values of the impulse response are the eigenvalues of the system. And, the amplitudes of the impulse responses at different locations are the eigenvectors of the system. If one assumes that the random decrement signatures represent the impulse response functions of the system, then the frequencies, dampings and relative amplitudes of the random decrement signatures may be used to represent the eigenvalues and eigenvectors of the system.

To accurately retrieve the eigenvalues and the eigenvectors, a time domain curve fitting procedure is applied to the random decrement signatures of the structure. First, the frequency and damping value of a random decrement signature are determined using the auto-regression method. After the frequency and damping are determined, the random decrement signatures are curve fitted with the following expression to determine the amplitudes of the signatures.

$$x(t) = \alpha_o + \sum_{i=1}^{M} \alpha_i e^{-\omega_i \zeta_i t} \sin(\omega_i t + \phi_i)$$

where ω_i and ζ_i are natural frequency and damping ratio of the i-th mode of the system. α_i and ϕ_i are the amplitude and phase angle. Again the curve fitting procedure uses the least square method.

4.3 Computer Program Development

A computer program was developed to implement the System Identification Technique illustrated in Figure 2. The Program includes a frequency domain curve fitting program, a random decrement program, a time domain curve fitting program and a system identification program. The random decrement program, written in Z80 Assembly language, is implemented in a CROMEMCO microcomputer. The resulting random decrement signature is transferred to the UNIVAC 1180 computer, where the other three programs are located, for subsequent processing.

The input to the frequency domain curve fitting program is the experimental transfer function which is collected using a NICOLET FFT Spectrum analyzer in which many instantaneous transfer functions are averaged. The averaged transfer function is transferred to the UNIVAC computer through an

interface microcomputer system. When the frequency domain curve fitting program receives the experimental transfer function from the spectrum analyzer and the time domain curve fitting program receives random decrement signatures of a structure from the random decrement microcomputer, both programs reduce the input data to yield the system's eigenvalues and eigenvectors. Then, the system identification program will pick up these eigenvalues and eigenvectors and reduces them to the system's [M][C][K] matrices.

4.4 Performance Test of the Time Domain Algorithm

The time domain approach uses an auto-regressive curve fitting method to resolve frequencies and damping values of a multidegree-of-freedom signal simultaneously. It was successfully tested with theoretical data of the type:

$$f(t) = \sum_{k=M}^{M} A_k e^{-\gamma_k t} \cos\omega_k t + B_k e^{-\gamma_k t} \sin\omega_k t, \qquad M = 3$$

The signal simulates the free decay response of a structure or the random decrement signature of the structural random response. Given various values of γ_k, ω_k, the time function f(t) is fed into the program. The program then resolves the frequencies and dampings from the time function f(t). The results are compared with the originally given values of frequencies and dampings. Many cases have been tested including different sampling rates, time lengths and modal separations (Table 1). The program performs very well in all theoretical cases.

Table 1

Theoretical Test Cases of the Time Domain Program

Input frequencies (Normalized to Sampling Rate)			Damping Ratio	Resolved frequencies (Normalized to Sampling Rate)			Damping Ratio
.03	.05	.07	.01	.03	.05	.07	.01
.15	.25	.35	.01	.15	.25	.35	.01
.08	.11	.14	.01	.08	.11	.14	.01
.10	.13	.16	.01	.10	.13	.16	.01
.15	.18	.21	.01	.15	.18	.21	.01
.20	.30	.40	.01	.20	.30	.40	.01
.05	.10	.15	.01	.05	.10	.15	.01
.08	.13	.18	.01	.08	.13	.18	.01
.15	.20	.25	.01	.15	.20	.25	.01

Due to the numerical truncation error plus the randomness of the real system, it is necessary to test the performance of the time-domain eigenvalue retrieving algorithm under noisy condition. A few test cases have been conducted whose results are presented below.

A theoretical signal which consists of three sinusoidal waves with frequencies 1456.3, 2427.2, 3398.1 Hz and damping ratios 1% for all three modes was convolved with a random white noise signal collected from an analog noise generator with a sampling rate of 9708.74 Hz. The result simulates the random response of a structure. After the auto-regression of the random decrement signature, the frequencies and damping ratios were resolved. The accuracies in the frequency calculation for all three modes are very good, all within 1%. However, the calculations of the damping ratios are less accurate. The error of the damping ratio of the first mode is 10%, second mode 15%, and third mode 85%. This is due to the fact that the added noise is not a white noise so that it can not be completely removed by the random decrement process. The modal separations of this signal are considered high. The three frequencies are at 15%, 25% and 35% of the sampling rate.

In the cases where many modes can not be resolved simultaneously, filtering process helps reduce the number of modes and improve the accuracy of the eigenvalue retrieval. A signal of 291.26 Hz, 485.44 Hz, 679.61 Hz (3%, 5%, 7% of the sampling rate) and damping ratio 1% was convolved with the random analog noise and filtered with filter band pass from 4.5% to 5.5% of the sampling rate. The filtered signal contains the dominate mode of 485.44 Hz. Other spectral modes attribute to the filter and the noise. When the three mode auto-regression algorithm was applied to the filtered signature, the

485.44 Hz distinct mode was picked out and the other two modes were used as error compensation. Due to the presence of the noise, the frequency and damping ratio obtained by using auto-regression method depends on the sampling rate and the number of data points used. Based on previous experimental experience, optimum sampling rate was found to be 3.5 - 7 times the frequency of interest and optimum number of data points was near 128. Using a sampling rate 3.33 times the frequency, the number of data points 128, the above filtered signal was resolved by the three mode auto-regression algorithm. This resulted in a frequency 482.86 Hz and damping ratio of 1.025%. Compared to the theoretical value, the frequency has 1% accuracy and the damping ratio 1% accuracy. Hence we believe the time domain algorithm accurately resolves the frequency and damping values of a multidegree-of-freedom system.

4.5 Performance Test of the Frequency Domain Algorithm

The frequency domain curve fitting program has successfully tested with theoretical frequency response functions generated by the following formula:

$$F(s) = \sum_{k=-M}^{M} \frac{a_k}{s - p_k}$$

Initially, the eigenvalues p_k and the residues a_k were assigned. The generated frequency response functions were fed into the frequency domain curve fitting program. The program resolved the residues and poles a_k, p_k of each mode. These values when compared to the original assigned values are very accurate.

Detailed testing results are referred to Appendix II.

4.6 Performance Test of the System Identification Algorithm

In order to demonstrate the ability of the computer program to retrieve the system identification parameters from theoretical response data, a simple computer experiment was conducted. Simple spring mass systems as illustrated in Figures 3, 4, 5 were analyzed. The theoretical response to a random loading was calculated for known values of mass, stiffness, and damping values. The system's eigenvalues and eigenvectors were then retrieved using the frequency domain technique with the theoretical response as input. Mass, stiffness, and damping matrices were determined using the System identification algorithm and compared with the original input values. Excellent agreement was obtained for all 3 cases studied. This demonstrated that the technique can accurately retrieve the system identification parameter even for large variations in mass, stiffness and damping parameters.

5. Analog Computer Experiment

In order to further demonstrate the feasibility of retrieving the System Parameters from response data, the analog computer was used to simulate response from real systems. An analog computer system was used to simulate the dynamic response of a two-degree-of-freedom spring-mass-dashpot system as shown in Figure 4. A schematic of the analog setup is shown in Figure 6. System input parameters can be easily adjusted by changing the resistor values of the potentiometers in the analog computer circuit. The response signals of the analog computer contains circuit noise which simulates the natural white noise contained in the dynamic responses of the real system.

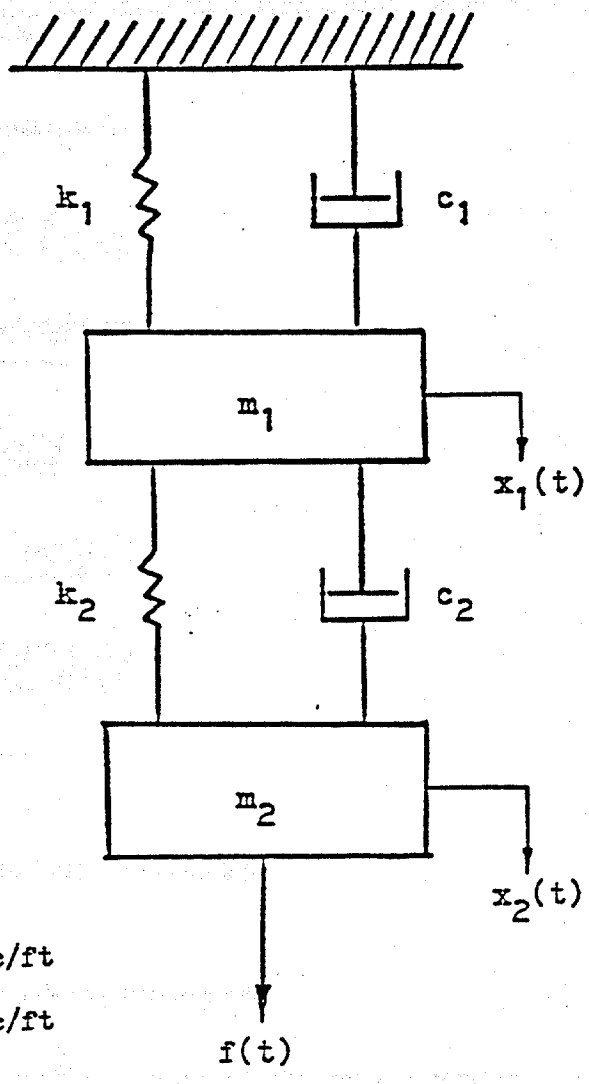

$m_1 = 1.0$ slug

$m_2 = 2.0$ slugs

$k_1 = 301.5$ lb/ft

$k_2 = 26535.0$ lb/ft

$c_1 = 0.1234$ lb.sec/ft

$c_2 = 2.6$ lb.sec/ft

Fig. 3 Two-degrees-of-freedom system with Well-Separated Modes (Model 1)

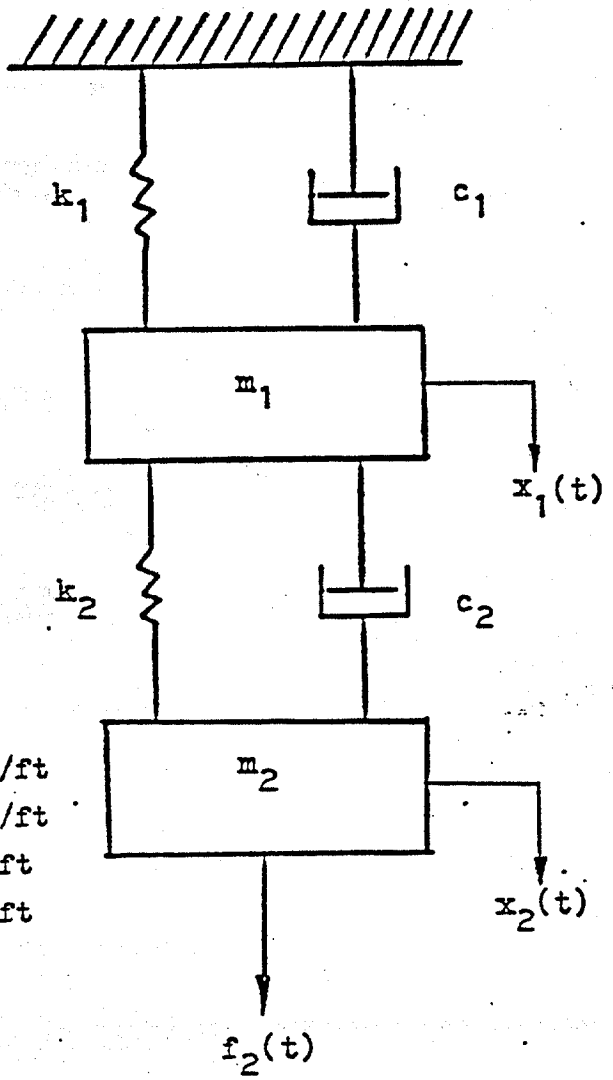

m_1 = 20.0 slugs
m_2 = 1.0 slug
c_1 = 10.135 lb.sec/ft
c_2 = 2.565 lb.sec/ft
k_1 = 10221.897 lb/ft
k_2 =490.919 lb/ft

Fig. 4 Two-degrees-of-freedom system with Closely-Spaced Modes (Model 2).

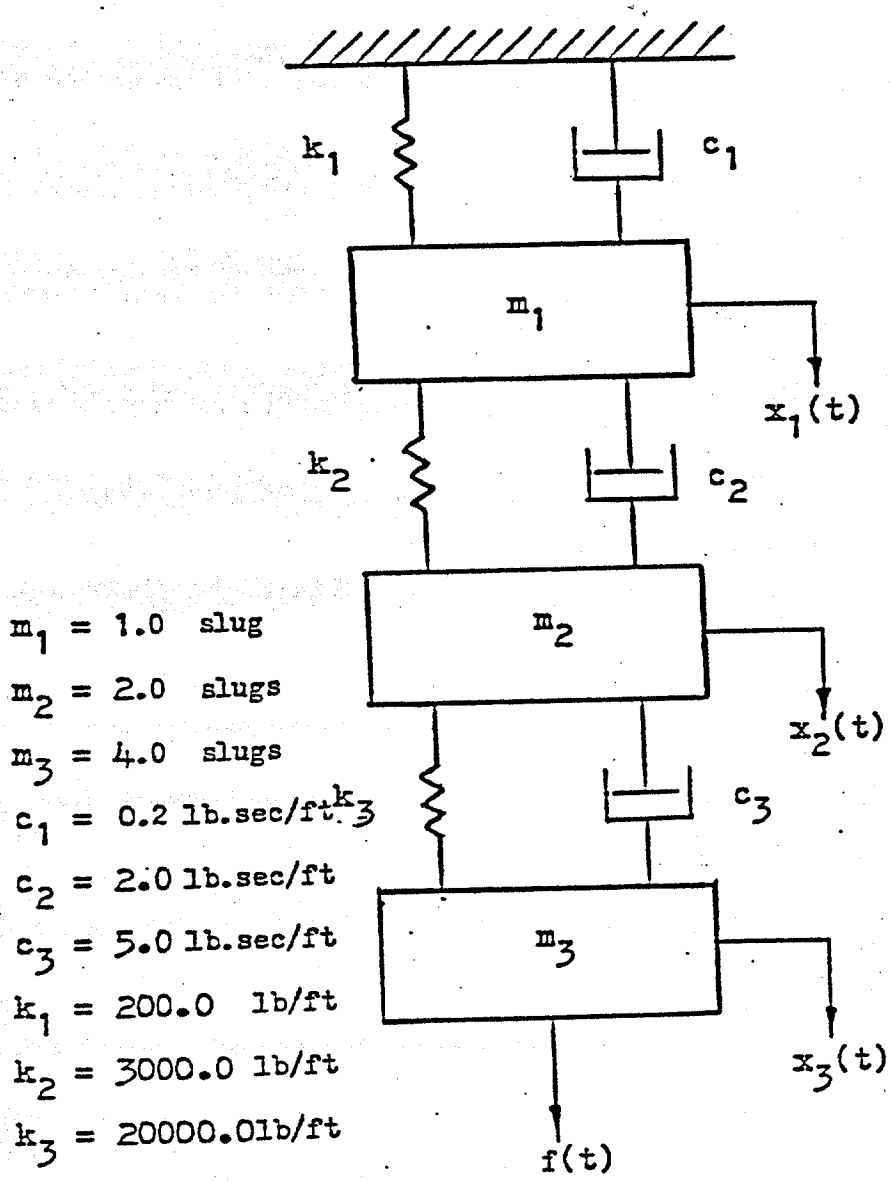

Fig. 5 Three-degrees-of-freedom system (Model 3).

The dynamic equations of the spring-mass-dashpot system of Fig. 4 are

$$\ddot{x}_1 = -\frac{c_1 + c_2}{m_1}\dot{x}_1 + \frac{c_2}{m_1}\dot{x}_2 - \frac{k_1 + k_2}{m_1}x_1 + \frac{k_2}{m_1}x_2$$

$$\ddot{x}_2 = \frac{c_2}{m_2}\dot{x}_1 - \frac{c_2 + c_3}{m_2}\dot{x}_2 + \frac{k_2}{m_2}x_1 - \frac{k_2 + k_3}{m_2}x_2 + \frac{f(t)}{m_2}$$

where m_1, m_2 are masses, c_1, c_2, c_3 damping constants, k_1, k_2, k_3 stiffness, $f(t)$ is the input forcing function at mass 2. Using k_1 = 1500 lb/ft, k_2 = 6000 lb/ft, k_3 = 1500 lb/ft, m_1 = 4 slugs, m_2 = 8 slugs, c_1 = 10 lb-sec/ft, c_2 = 20 lb-sec/ft, c_3 = 30 lb-sec/ft, and applying a random input forcing function to mass 2, the displacement transfer function at mass 1 and 2 were obtained as shown in Fig. 7 and Fig. 8 respectively. These transfer functions were fed into the frequency domain eigenvalue retrieving program from which the residues and poles of the system transfer functions were found as shown in Table 2.

Table 2

Poles and residues of the velocity transfer functions

		(1st stage damage) 1st Mode	2nd Mode
$\dot{x}_1$	Frequency (rad/sec)	15.78	50.22
	Damping Ratio	0.1802	0.1551
	Residues	0.04227 + i0.006686	-0.04111 - i0.004233
$\dot{x}_2$	Frequency (rad/sec)	15.79	50.23
	Damping Ratio	0.1796	0.1541
	Residues	0.04426 + i0.008879	0.01880 - i0.000418

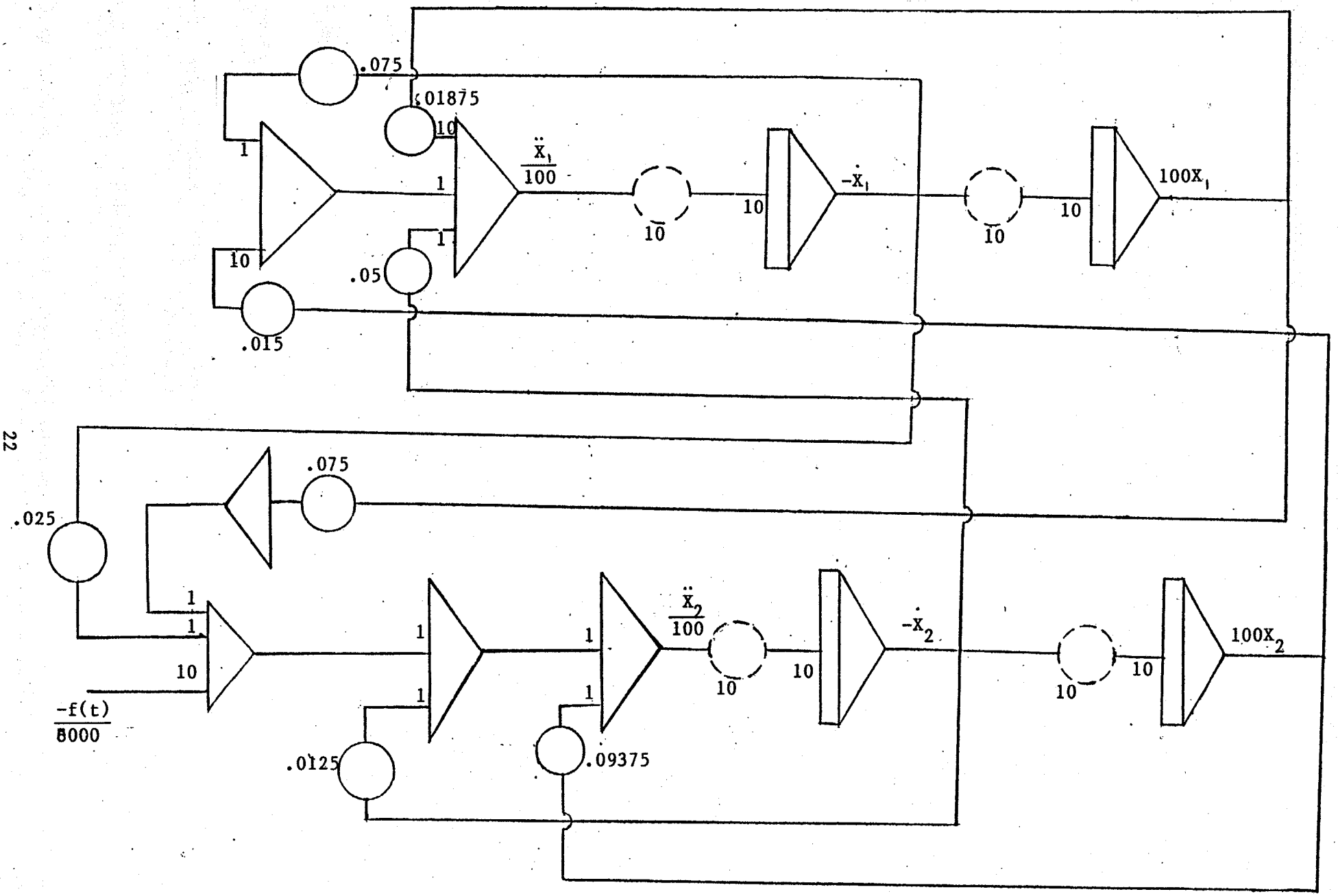

Fig.6 Analog Computer setup

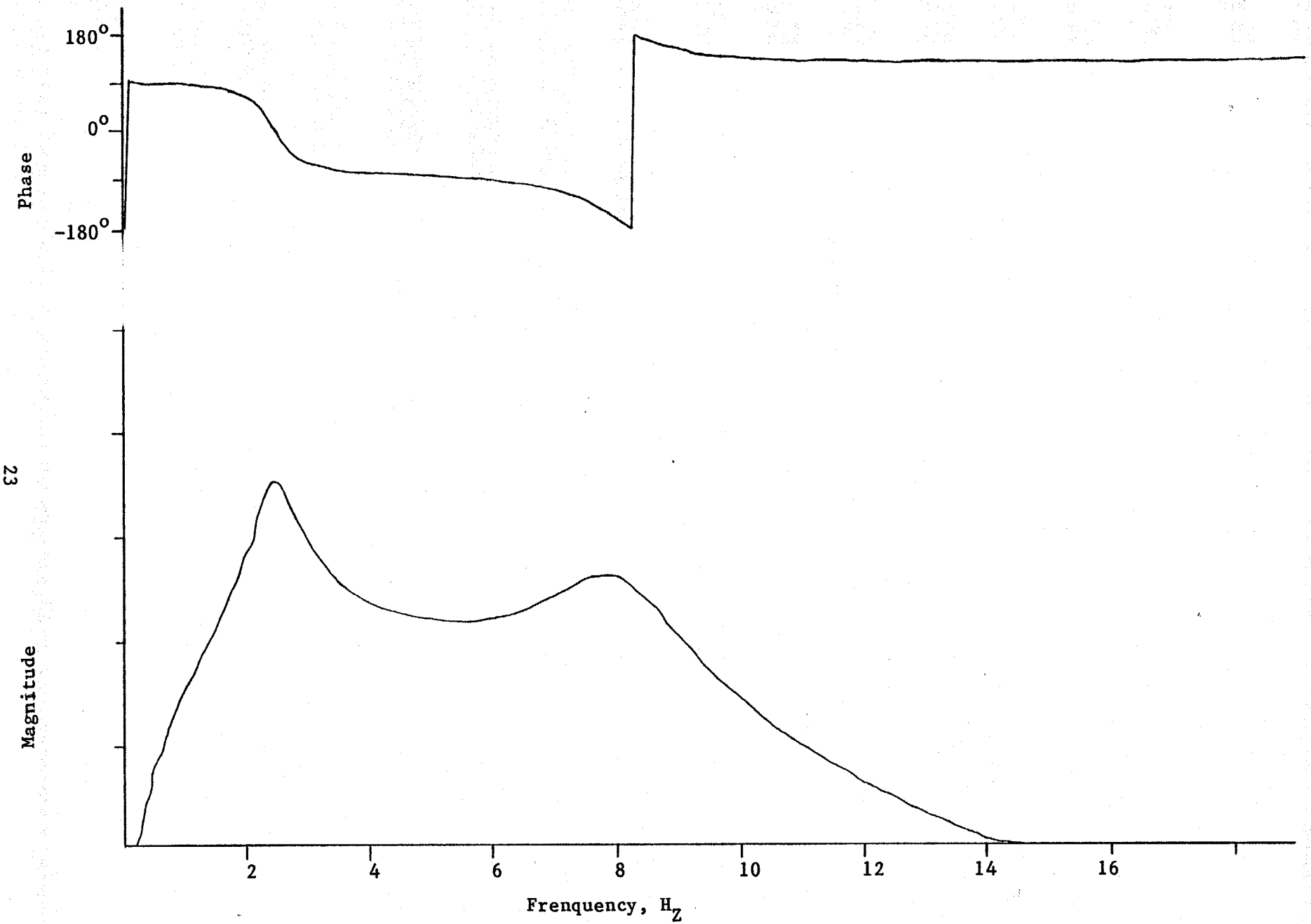

Fig. 7 Velocity Transfer Function of mass 1 with force applied at mass 2

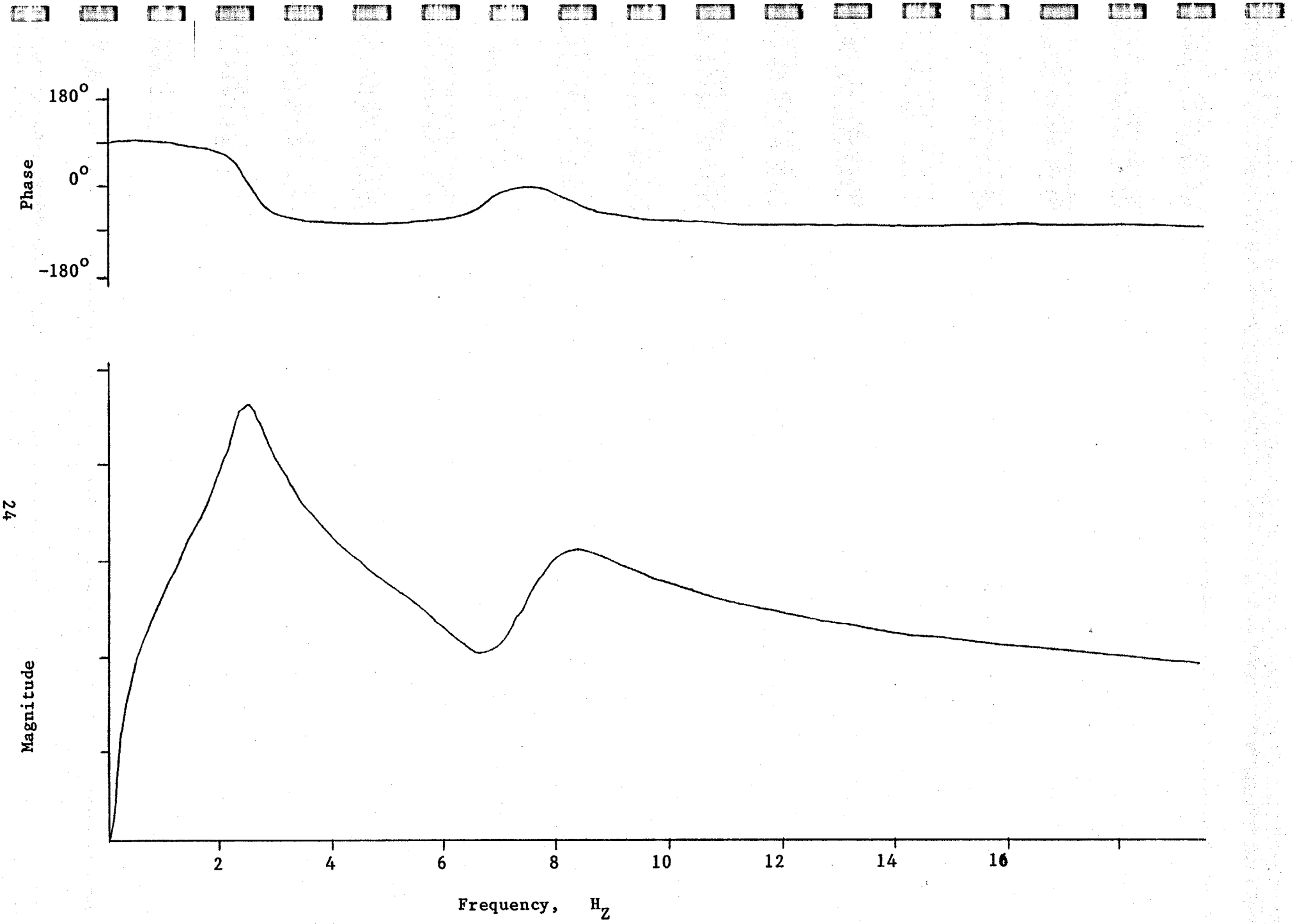

Fig. 8 Velocity Transfer Function of mass 2 with force applied at mass 2

When the eigenvalues and eigenvectors were fed into the system identification program, the system's [M][C][K] matrices were identified, as shown below

$$M = \begin{bmatrix} 3.944 & -0.00492 \\ -0.000284 & 7.88 \end{bmatrix} \quad \text{slugs}$$

$$C = \begin{bmatrix} 28.4 & -19.6 \\ -19.6 & 50.8 \end{bmatrix} \quad \text{lb-sec/ft}$$

$$K = \begin{bmatrix} 7477 & -5933 \\ -5933 & 7452 \end{bmatrix} \quad \text{lb/ft}$$

The exact values of the system's [M][C][K] matrices from theoretical calculations are

$$M_{theo.} = \begin{bmatrix} 4.0 & 0 \\ 0 & 8.0 \end{bmatrix} \quad \text{slugs}$$

$$C_{theo.} = \begin{bmatrix} 30.0 & -20.0 \\ -20.0 & 50.0 \end{bmatrix} \quad \text{lb/sec/ft}$$

$$K_{theo.} = \begin{bmatrix} 7500 & -6000 \\ -6000 & 7500 \end{bmatrix} \quad \text{lb/ft}$$

The comparison between the identified and theoretical values of the [M][C][K] matrices are within 5%. This again demonstrated the ability of the System Identification Technique to accurately retrieve [M][C][K] matrices from the response data.

In order to demonstrate the ability to detect system changes from simulated damage, three stages of damage were simulated. Stage 1 was considered to have characteristics of the system just analyzed. Stages 2 and 3 were as given below:

Stage 2 Damage: $m_1 = 4.0$ slugs, $m_2 = 8.0$ slugs

$c_1 = 40$ lb-sec/ft, $c_2 = 20.0$ lb-sec/ft, $c_3 = 30.0$ lb-sec/ft

$k_1 = 1500$ lb/ft, $k_2 = 3000$ lb/ft, $k_3 = 1500$ lb/ft

Stage 3 Damage: $m_1 = 4.0$ slugs, $m_2 = 8.0$ slugs

$c_1 = 10$ lb-sec/ft, $c_2 = 20.0$ lb-sec/ft, $c_3 = 30.0$ lb-sec/ft

$k_1 = 1500$ lb/ft, $k_2 = 3000$ lb/ft, $k_3 = 1500$ lb/ft

The poles and residues of the velocity transfer functions for the 2nd and 3rd stages of damage are listed in table 3 and 4. The corresponding [M][C][K] matrices are shown below. Again it is demonstrated that the System Identification technique using the frequency domain algorithm can accurately retrieve the [M][C][K] matrices from response data. Moreover, changes simulating various stages of damage are detectable.

Table 3

Poles and Residues of the Velocity Transfer Functions

(2nd Stage Damage)

		1st Mode	2nd Mode
$\dot{x}_1$	Frequency (rad/sec)	15.89	50.58
	Damping Ratio	0.1088	0.1020
	Residues	0.04094 + i0.004655	-0.04089 - i0.004923
$\dot{x}_2$	Frequency (rad/sec)	15.89	50.56
	Damping Ratio	0.1092	0.1020
	Residues	0.04474 - i0.01735	0.01865 - i0.003211

Table 4

Poles and Residues of the Velocity Transfer Functions

(3rd Stage Damage)

		1st Mode	2nd Mode
$\dot{x}_1$	Frequency (rad/sec)	15.85	37.88
	Damping Ratio	0.1109	0.1359
	Residues	0.03958 + i0.004973	0.03944 - i0.006832
$\dot{x}_2$	Frequency (rad/sec)	15.85	37.87
	Damping Ratio	0.1103	0.1349
	Residues	0.04697 + i0.004429	0.01645 - i0.004332

2nd stage damage:

$$M_{theo.} = \begin{bmatrix} 4.0 & 0 \\ 0 & 8.0 \end{bmatrix} \quad \text{slugs}$$

$$C_{theo.} = \begin{bmatrix} 60 & -20.0 \\ -20.0 & 50.0 \end{bmatrix} \quad \text{lb-sec/ft}$$

$$K_{theo.} \begin{bmatrix} 7500 & -6000 \\ -6000 & 7500 \end{bmatrix} \quad \text{lb/ft}$$

$$M = \begin{bmatrix} 3.944 & -0.001989 \\ -0.00334 & 7.934 \end{bmatrix} \quad \text{slugs}$$

$$C = \begin{bmatrix} 59.139 & -19.428 \\ -19.428 & 49.205 \end{bmatrix} \quad \text{lb-sec/ft}$$

$$K = \begin{bmatrix} 7494.0 & -5963.8 \\ -5963.8 & 7520.8 \end{bmatrix} \quad \text{lb/ft}$$

3rd stage damage:

$$M = \begin{bmatrix} 3.936 & -0.0117 \\ -0.0058 & 7.878 \end{bmatrix}$$

$$C = \begin{bmatrix} 28.74 & -19.52 \\ -19.52 & 49.90 \end{bmatrix}$$

$$K = \begin{bmatrix} 4509 & -2970 \\ -2970 & 4511 \end{bmatrix}$$

$$M_{theo.} = \begin{bmatrix} 4.0 & 0 \\ 0 & 8.0 \end{bmatrix}$$

$$C_{theo.} = \begin{bmatrix} 30 & -20 \\ -20 & 50 \end{bmatrix}$$

$$K_{theo.} = \begin{bmatrix} 4500 & -3000 \\ -3000 & 4500 \end{bmatrix}$$

Time responses of the system were also investigated. Shown in Figs. 9 and 10 are the velocity time responses of $\dot{x}_1$ and $\dot{x}_2$, respectively, where the external forces and all other initial conditions are zero except initial displacement $x_1(0) = 0.15$ ft. Figs. 11 and 12 show the displacement time responses $x_1(t)$, $x_2(t)$ when a constant force $f_2 = 1222.4$ lb was applied to mass 2 and the initial conditions were set at $x_1(0) = -0.80$ ft, $x_2(0) = +0.80$ ft. Figs. 13 and 14 are the displacement time responses $x_1(t)$, $x_2(t)$ when a constant force $f_1 = 611.6$ lb was applied to mass 1 with initial conditions $x_1(0) = -0.80$ ft, $x_2(0) = 0.80$ ft. Using the time domain eigenvalue retrieving program, the frequencies, dampings and amplitudes of time response curves for the 3 stages of damage were found and are shown in tables 5, 6, and 7.

Normalized damping and stiffness matrices $[\tilde{C}]$, $[\tilde{K}]$ were found from the time responses. They are defined as the ratio of the actual damping and stiffness matrices to the mass matrices:

$$\tilde{C} = M^{-1}C, \quad \tilde{K} = M^{-1}K$$

The calculated $[\tilde{C}]$, $[\tilde{K}]$ and their corresponding theoretical values for the three stages of damage are listed below in Table 8.

The results demonstrate that the System Identification Technique using the time domain algorithm also accurately retrieves the [M][C][K] matrices, and changes simulating damage are detectable.

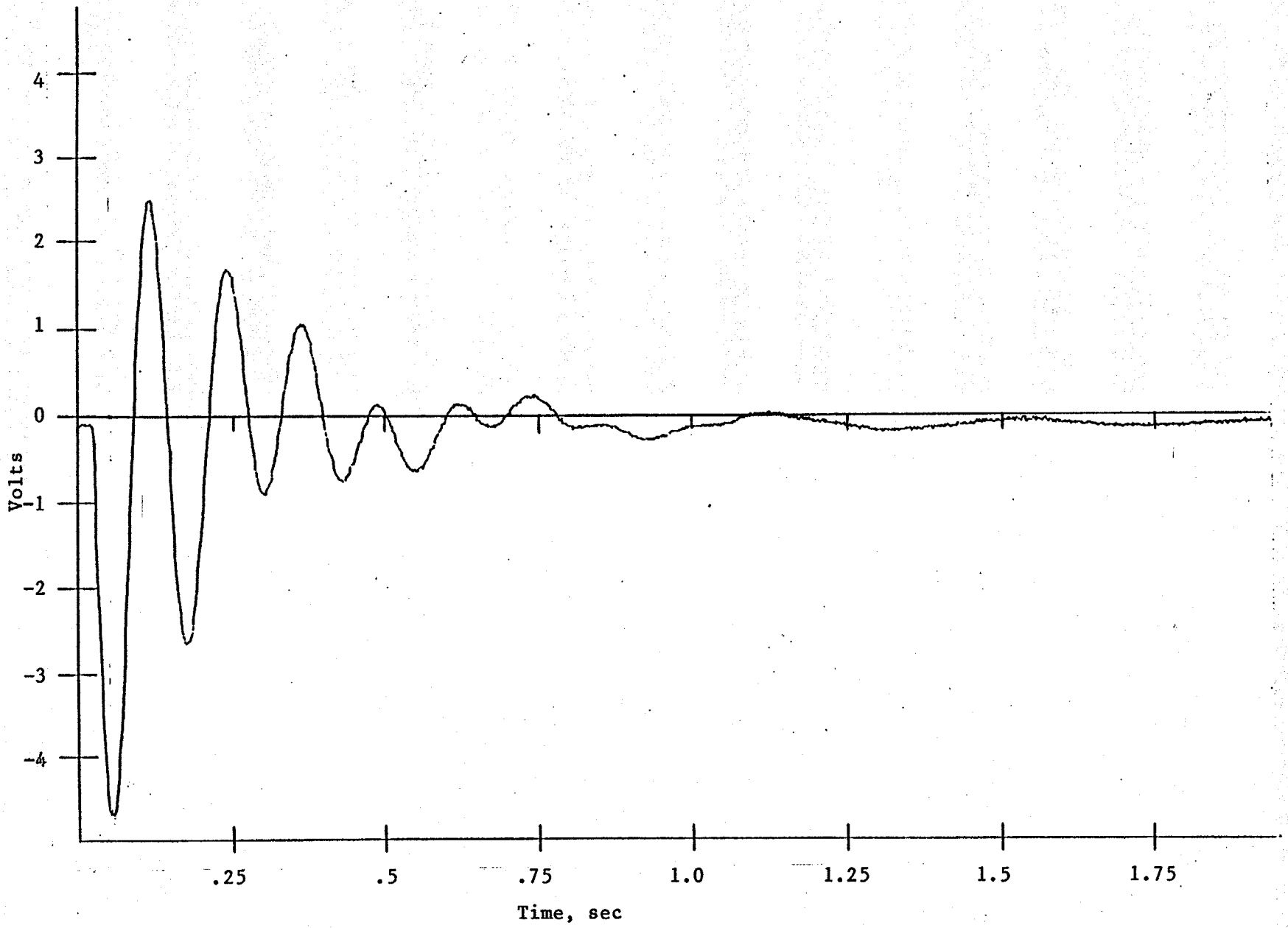

Fig. 9 Velocity time response at mass 1, with constant force at mass 2

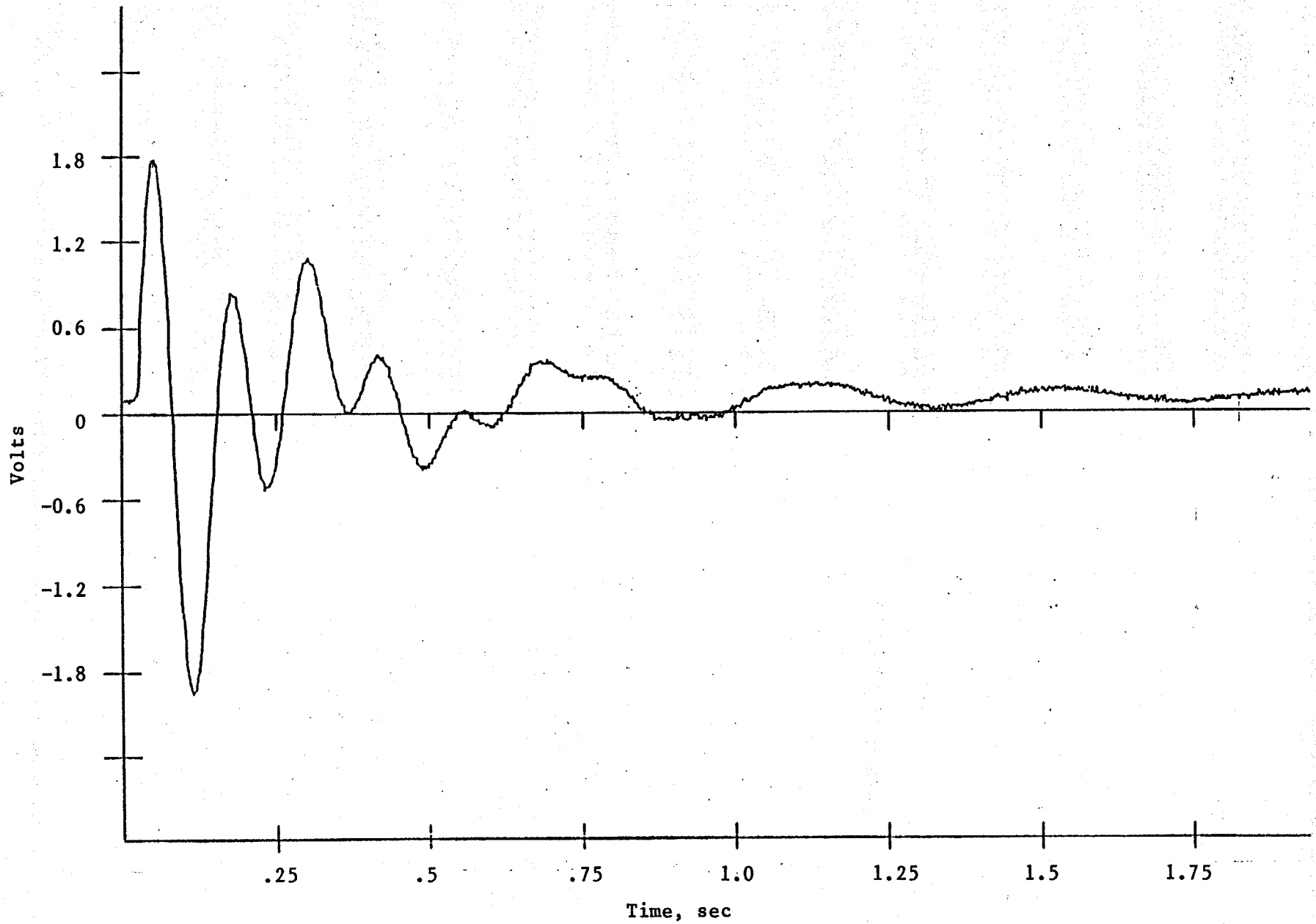

Fig. 10 Velocity time response at mass 2, with constant force at mass 2

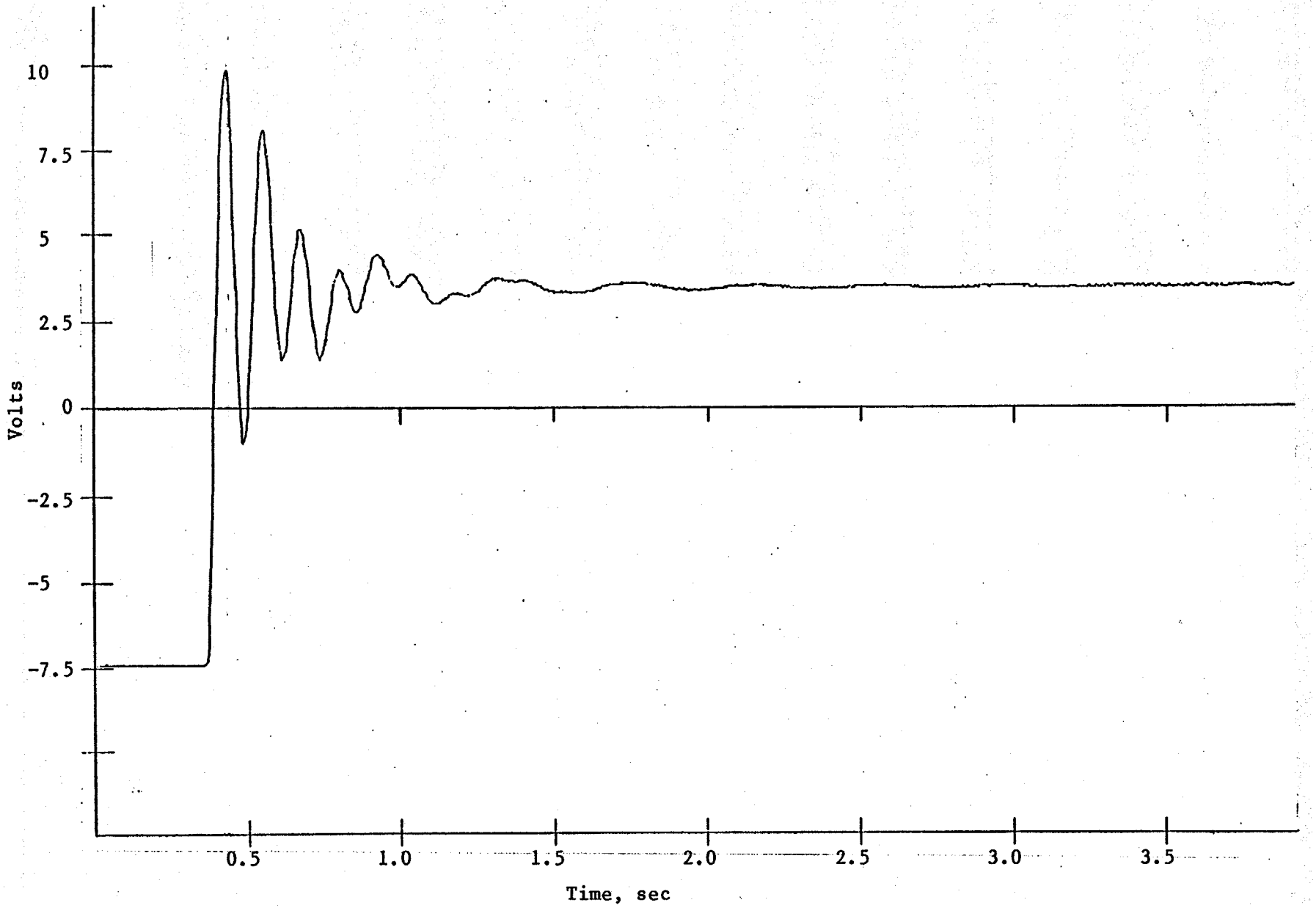

Fig. 11 Displacement time response at mass 1, with constant force at mass 2

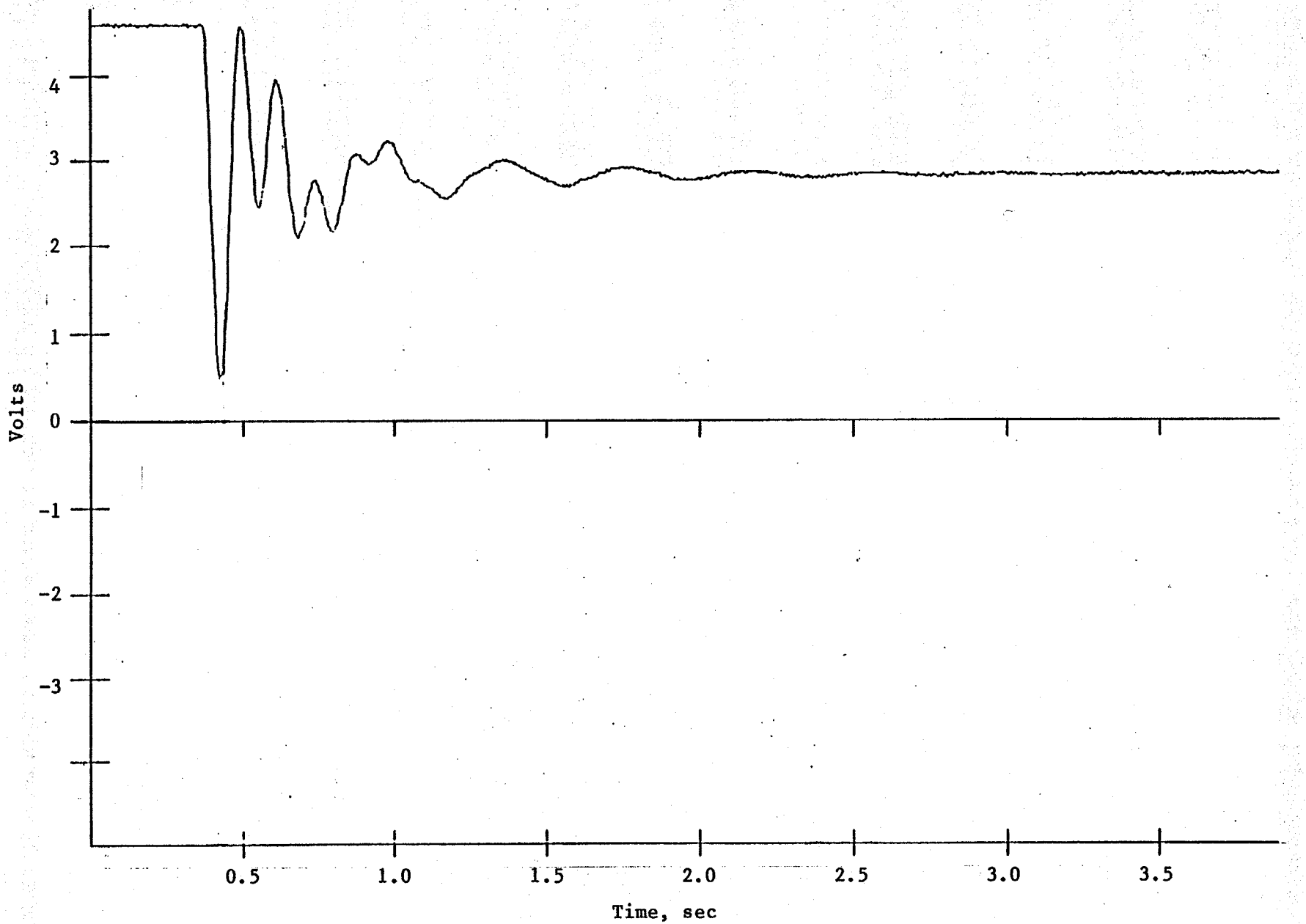

Fig. 12 Displacement time response at mass 2, with constant force at mass 2

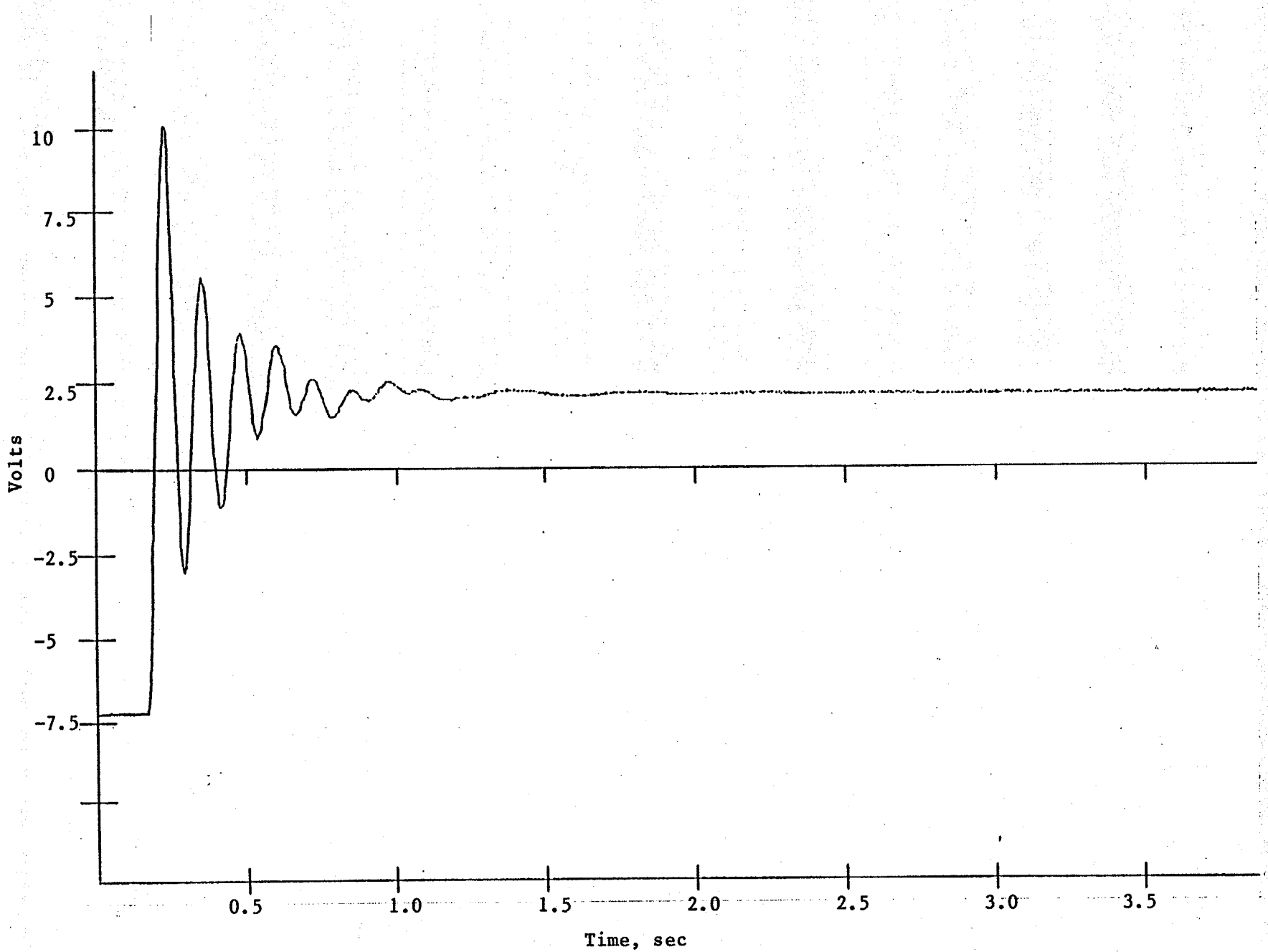

Fig. 13 Displacement time response at mess 1, with constant force at mass 1

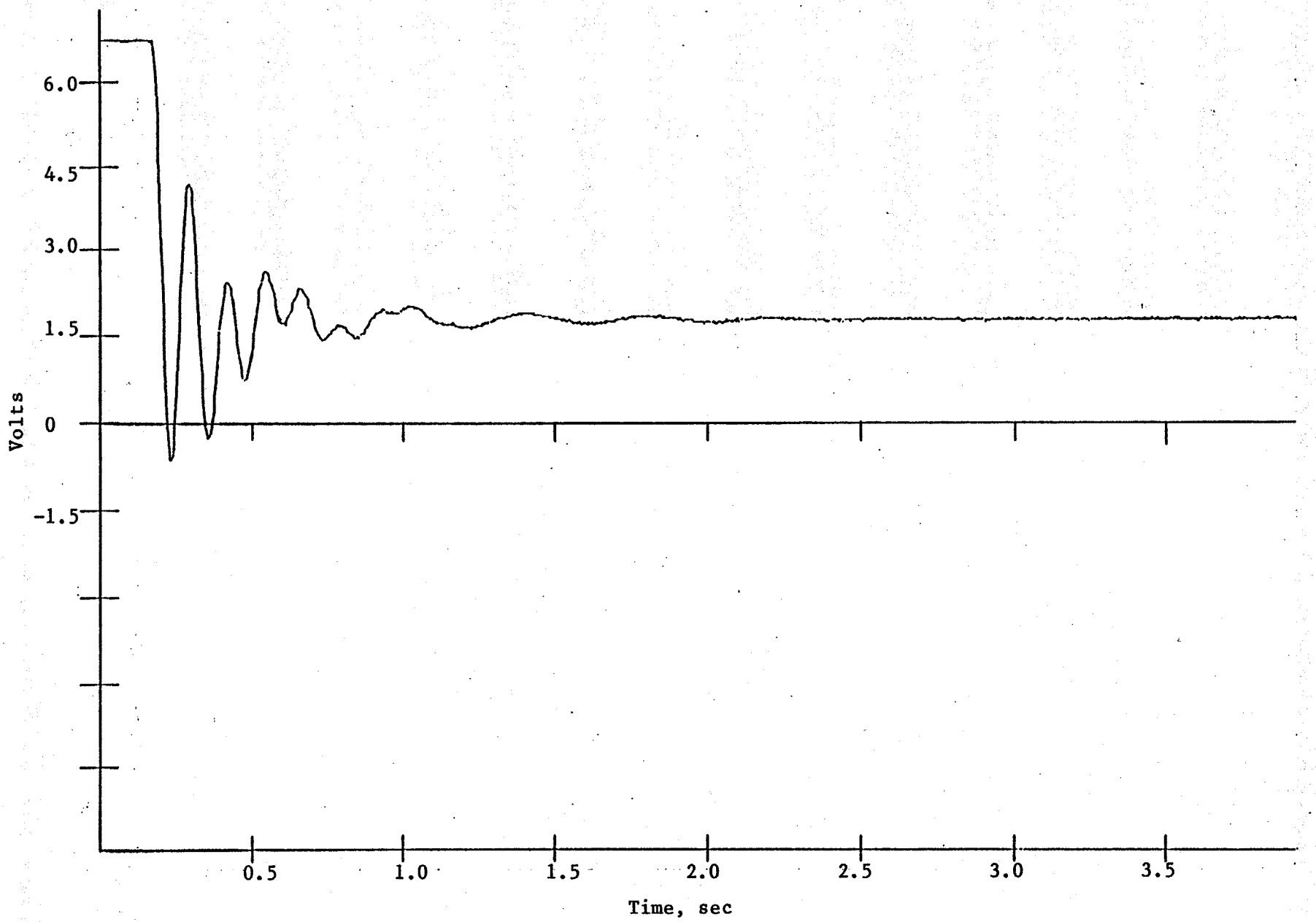

Fig. 14 Displacement time response at mass 2, with constant force at mass 1

Table 5

Frequencies, Dampings and Amplitudes of the

Time Responses

(1st Stage Damage)

Conditions	1st mode Freq. (Hz), Damping ratio, Amplitudes			2nd mode Freq. (Hz), Damping Ratio, Amplitudes		
$x_1(0) = 0.15$ ft						
$x_1(t)$	2.47	0.1151	-0.04332	8.03	0.1106	1.2689
$x_2(t)$	2.47	0.1082	-0.04266	8.03	0.1058	-0.4881
$x_1(0) = -0.80$ ft $x_2(0) = +0.80$ ft $f_1 = 611.6$ lb						
$x_1(t)$	2.52	0.1135	0.07164	8.04	0.1039	-1.0296
$x_2(t)$	2.49	0.1102	0.07285	7.99	0.1033	0.4597
$x_1(0) = -0.80$ ft $x_2(0) = +0.80$ ft $f_2 = 1222.4$ lb						
$x_1(t)$	2.48	0.1118	-0.1370	8.00	0.1029	-0.9267
$x_2(t)$	2.48	0.1108	-0.1457	8.00	0.1031	0.4256

Table 6

Frequencies, Dampings and Amplitudes of the

Time Responses

(2nd Stage Damage)

Conditions	1st mode Freq. (Hz), Damping ratio, Amplitudes			2nd mode Freq. (Hz), Damping Ratio, Amplitudes		
$x_1(0) = -0.80$ ft $x_2(0) = +0.80$ ft $f_1 = 611.6$ lb						
$x_1(t)$	2.46	0.1852	0.08358	7.93	0.1558	-1.0148
$x_2(t)$	2.46	0.1846	0.08270	7.95	0.1562	0.4461
$x_1(0) = -0.80$ ft $x_2(0) = +0.80$ ft $f_2 = 1222.4$ lb						
$x_1(t)$	2.46	0.1827	-0.1293	7.94	0.1555	-0.9344
$x_2(t)$	2.45	0.1843	-0.1456	7.97	0.1531	0.4066

Table 7

Frequencies, Dampings and Amplitudes of the

Time Responses

(3rd Stage Damage)

Conditions	1st mode Freq. (Hz), Damping ratio, Amplitudes			2nd mode Freq. (Hz), Damping Ratio, Amplitudes		
$x_1(0) = -0.80$ ft $x_2(0) = +0.80$ ft $f_1 = 611.6$ lb						
$x_1(t)$	2.47	0.1135	0.1006	5.98	0.1364	-1.0381
$x_2(t)$	2.48	0.1111	0.11167	5.99	0.1349	0.4348
$x_1(0) = -0.80$ ft $x_2(0) = +0.80$ ft $f_2 = 1222.4$ lb						
$x_1(t)$	2.46	0.1137	-0.1086	5.98	0.1359	-0.90167
$x_2(t)$	2.46	0.1138	-0.1276	5.97	0.1372	0.3837

Table 8

Normalized damping and stiffness matrices

	$\tilde{C}$		$\tilde{K}$		$\tilde{C}_{theo.}$		$\tilde{K}_{theo.}$	
1st stage damage	7.73	-4.57	1865	-1524	7.5	-5	1875	-1500
	-2.52	6.09	-732	933.8	-2.5	6.25	-750	937.5
2nd Stage damage	15.6	-3.98	1873	-1515	15	-5	1875	-1500
	-2.53	5.66	-738	932.6	-2.5	6.25	-750	937.5
3rd stage damage	7.41	-5.16	1119	-756	7.5	-5	1125	-750
	-2.42	6.36	-369	560.2	-2.5	6.25	-375	562.5

These results demonstrate that the System Identification Technique using the time domain algorithm also accurately retrieves the [M][C][K] matrices, and changes simulating damage are detectable.

6. The Cantilever Beam Experiment

6.1 Experimental Test

A cantilever beam was tested to verify that the system identification technique described in the previous section is equally effective for a continuous system. The beam, as shown in Figure 15, was excited with single and random impact near the end. Six accelerometers were attached to the beam at six equally spaced position. The transfer functions from the impact position to any accelerometer position was obtained by feeding the output acceleration signal and input forcing function into a spectrum analyzer: the Nicolet FFT analyzer. In the analyzer, the input and output signals were digitized and the Fast Fourier transform of the signals was performed. The instantaneous transfer functions were obtained by dividing the two spectra. Final transfer function was obtained by averaging over a series of instantaneous transfer functions. These transfer functions of various positions are shown in Figs. 16-21. Damages were introduced to the system. The first damage scenario was a one-fourth depth saw cut into the edge of the beam. Close examination of the results indicates that the higher frequency resonances/residues shift depends on the depth of the saw cut simulating a crack. The System Identification technique can detect the effects of the simulated cracks by changes in the [M][C][K] matrices.

7. NASTRAN Simulation

To provide a theoretical understanding of the effect of cracks, the dynamic behavior of a cantilever beam was studied. The frequency responses of

Material: Mild Steel

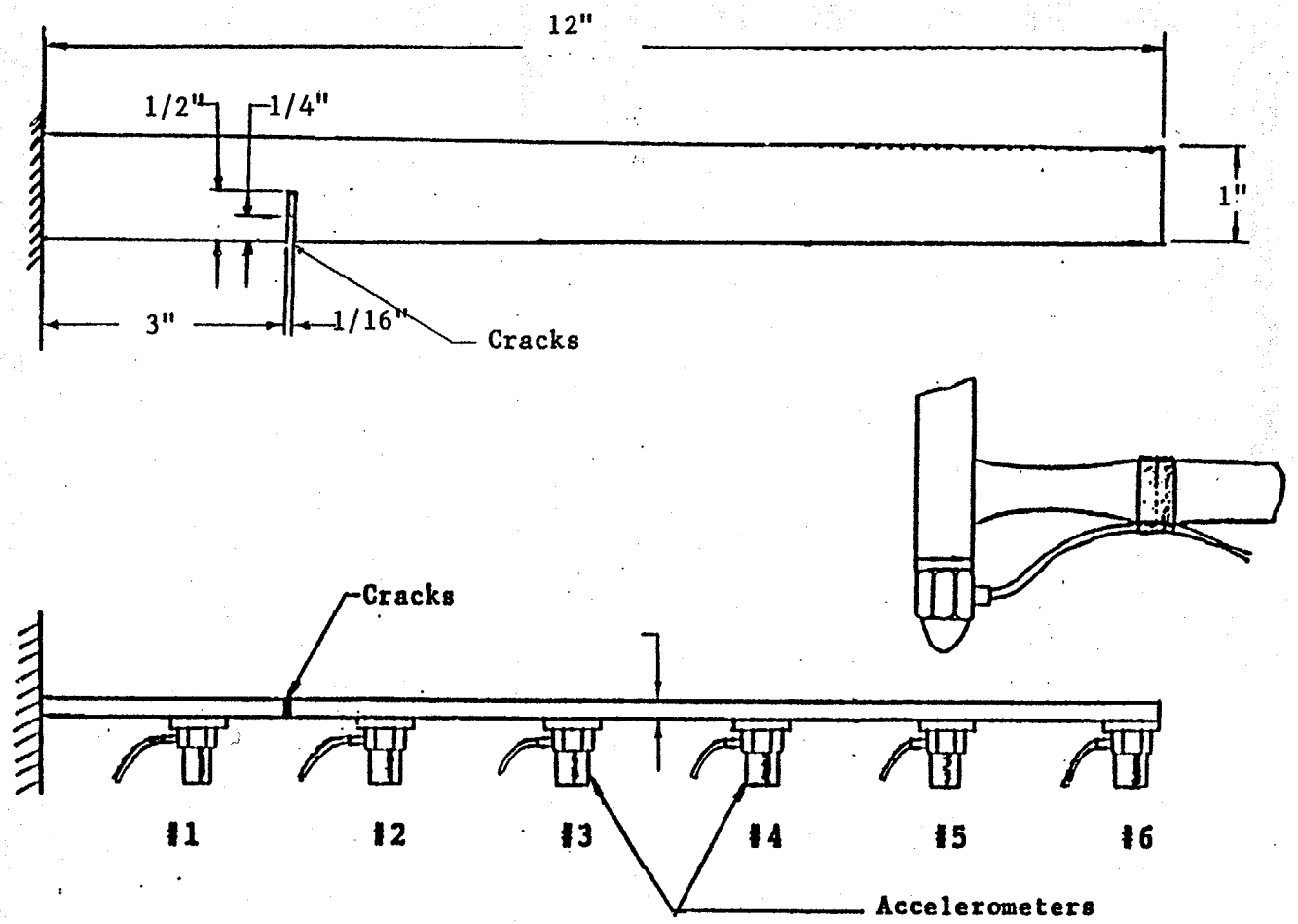

Fig. 15 The Cantilever Beam System

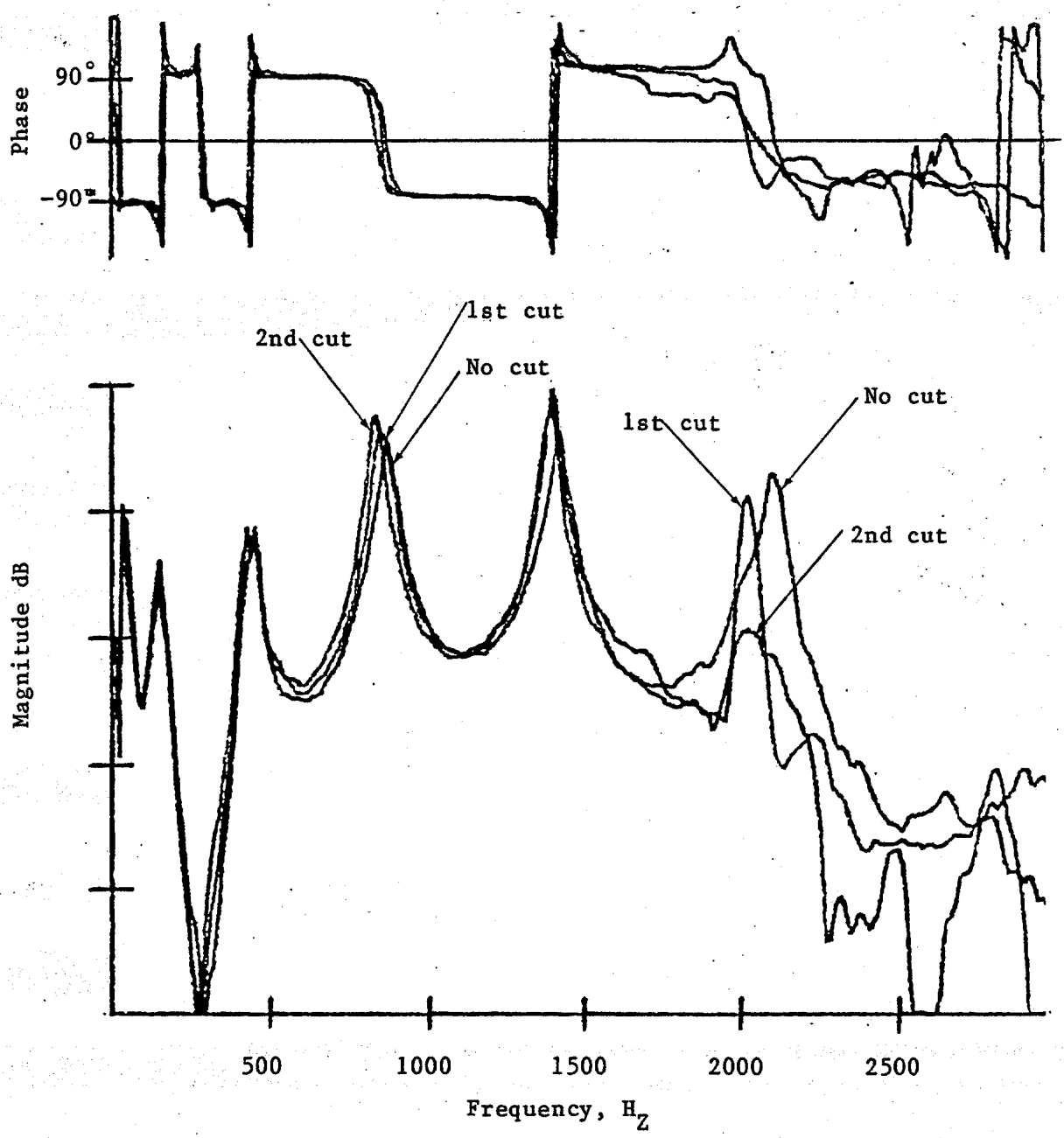

Fig. 16 Transfer Functions at location 1, with force at location 5

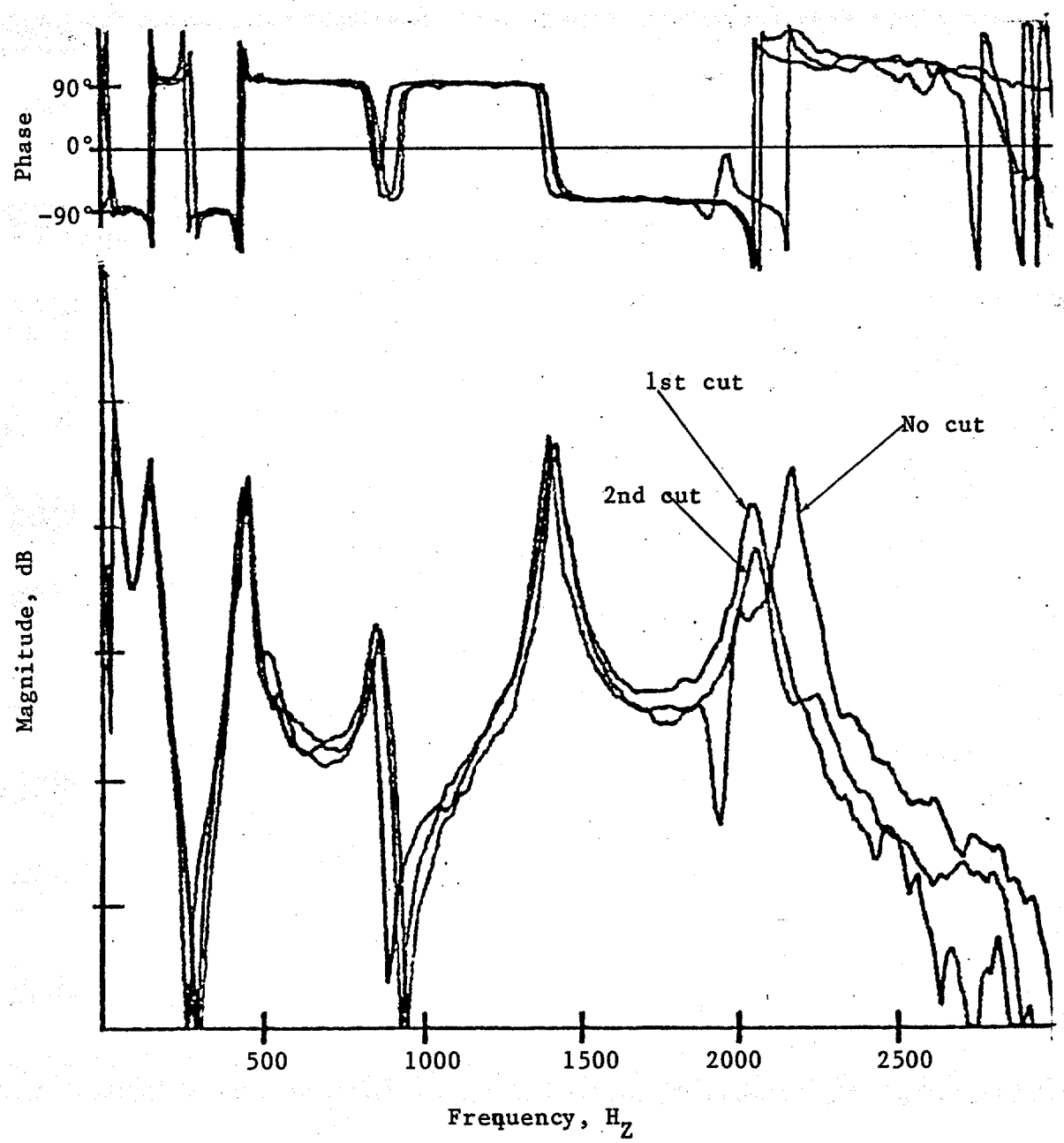

Fig. 17 Transfer Functions at location 2, with force at location 5

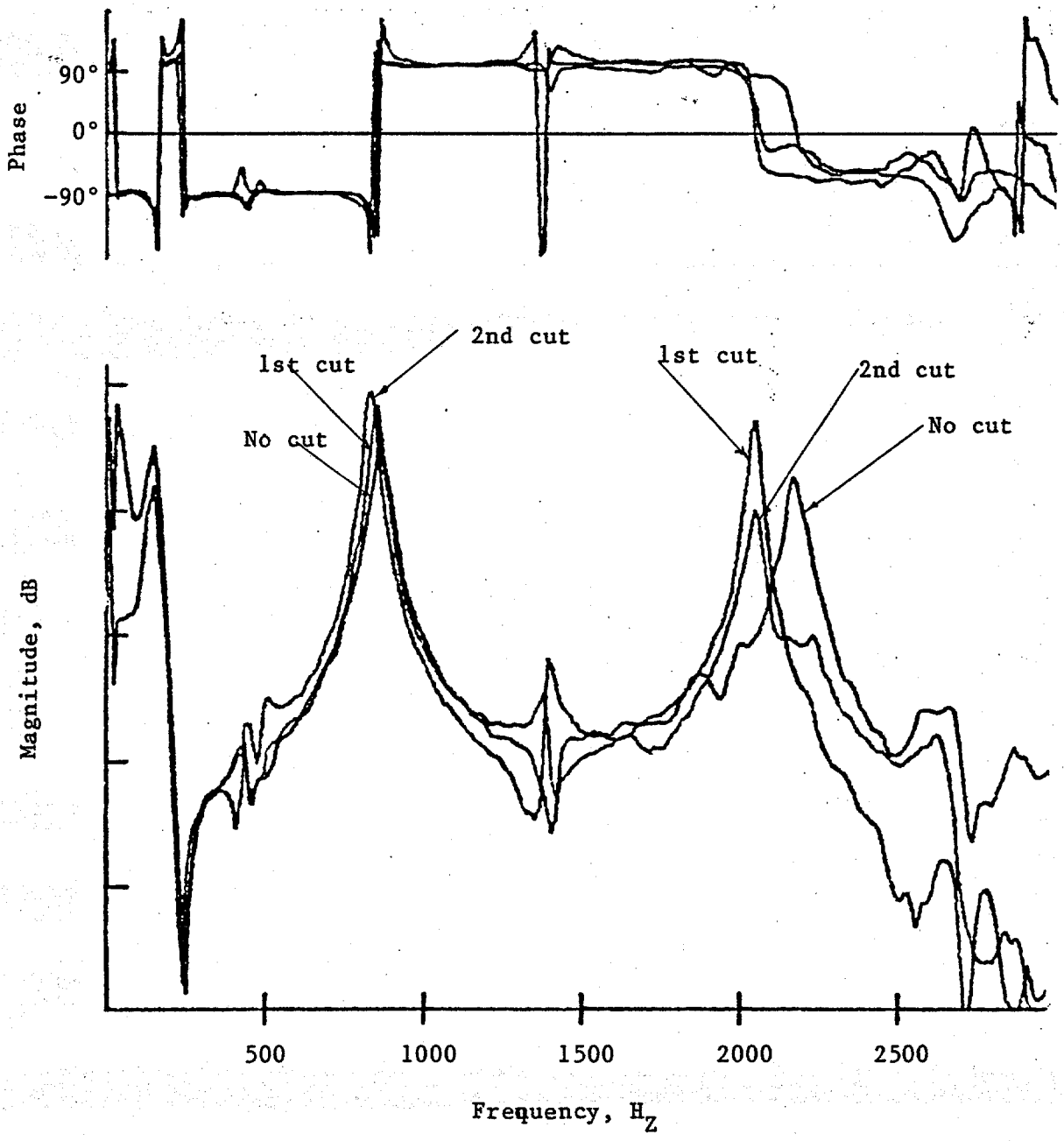

Fig. 18 Transfer Functions at location 3, with force at location 5

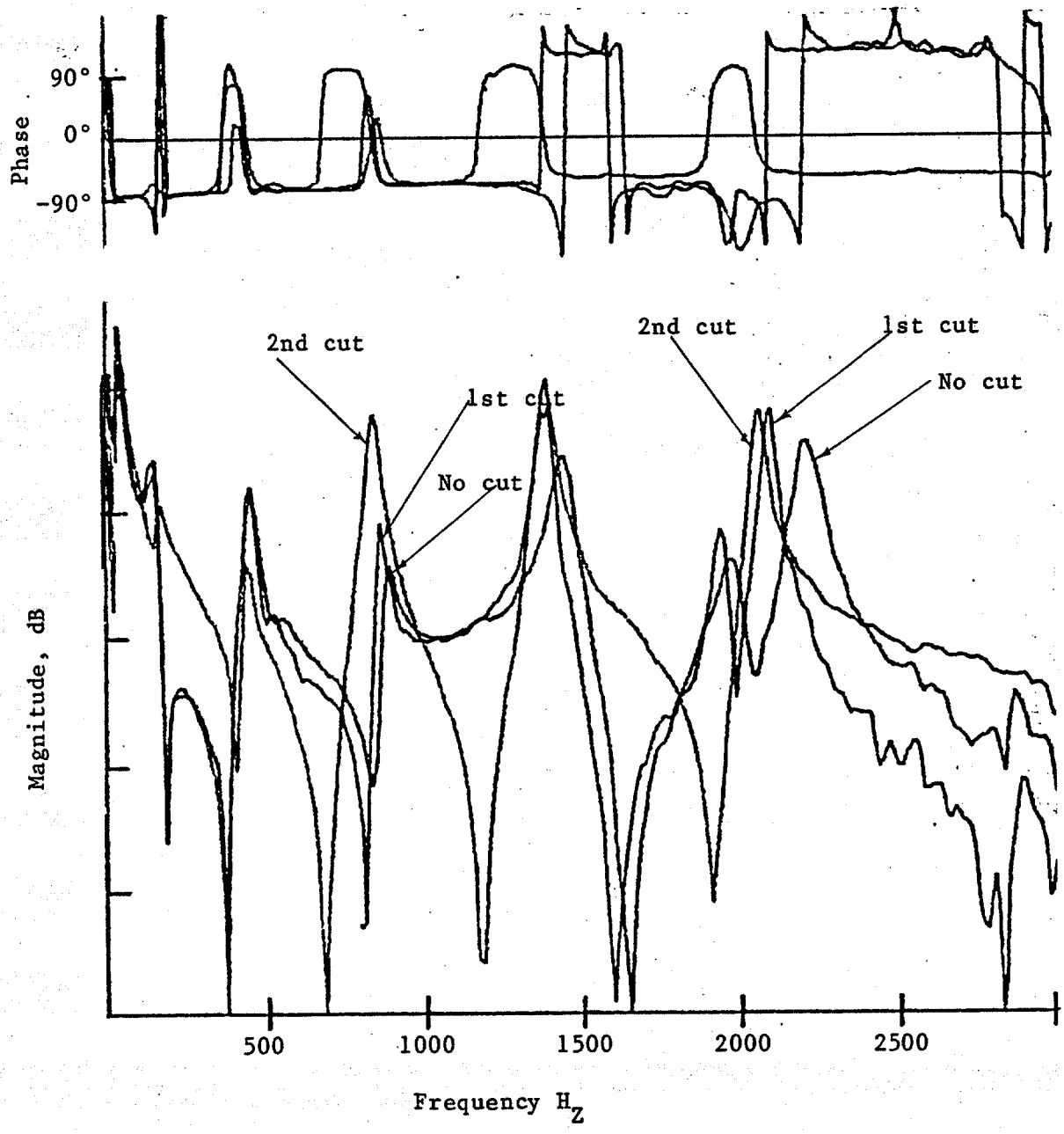

Fig. 19 Transfer Functions at location 4, with force at location 5

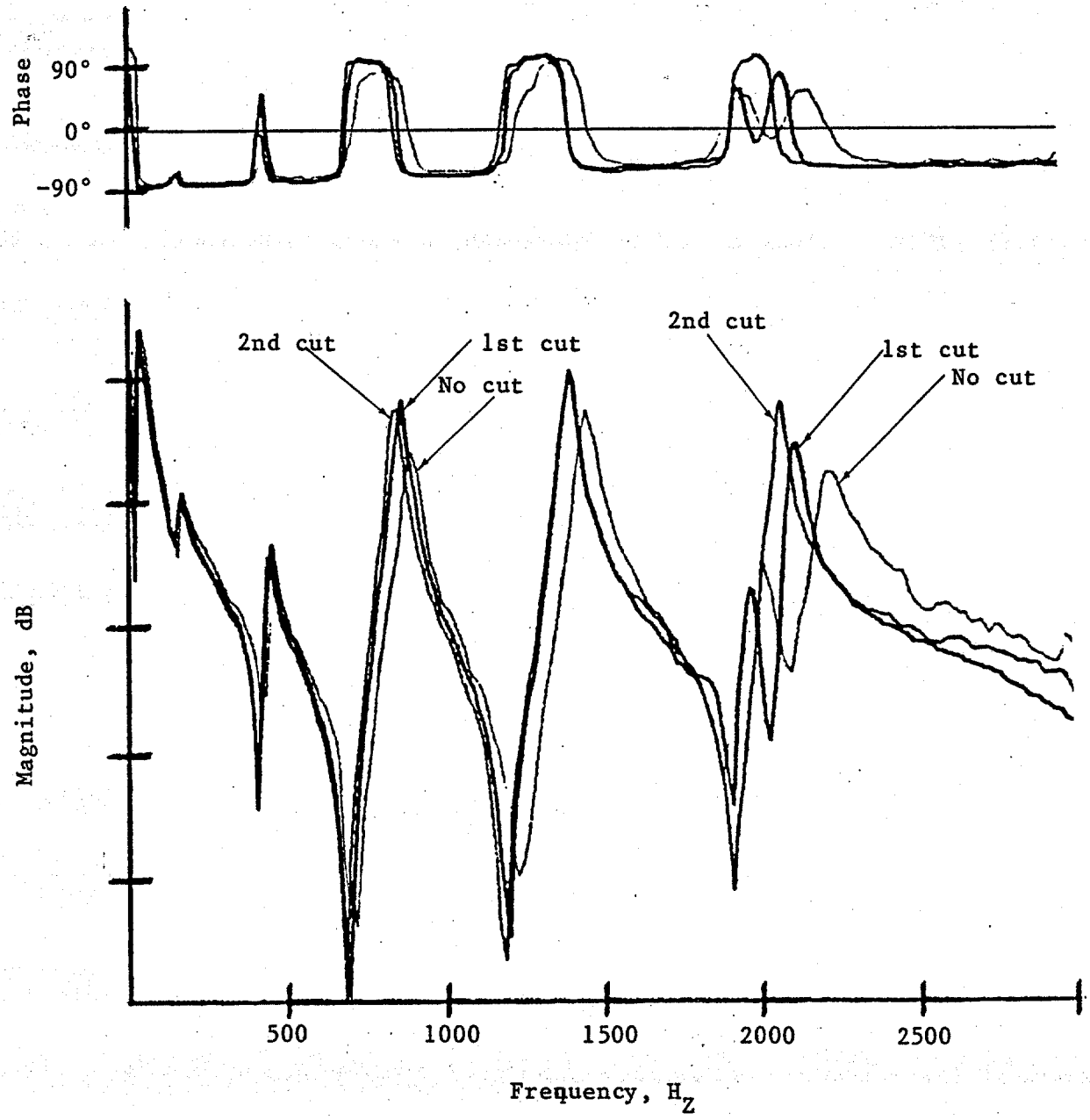

Fig. 20 Transfer Functions at location 5, with force at location 5

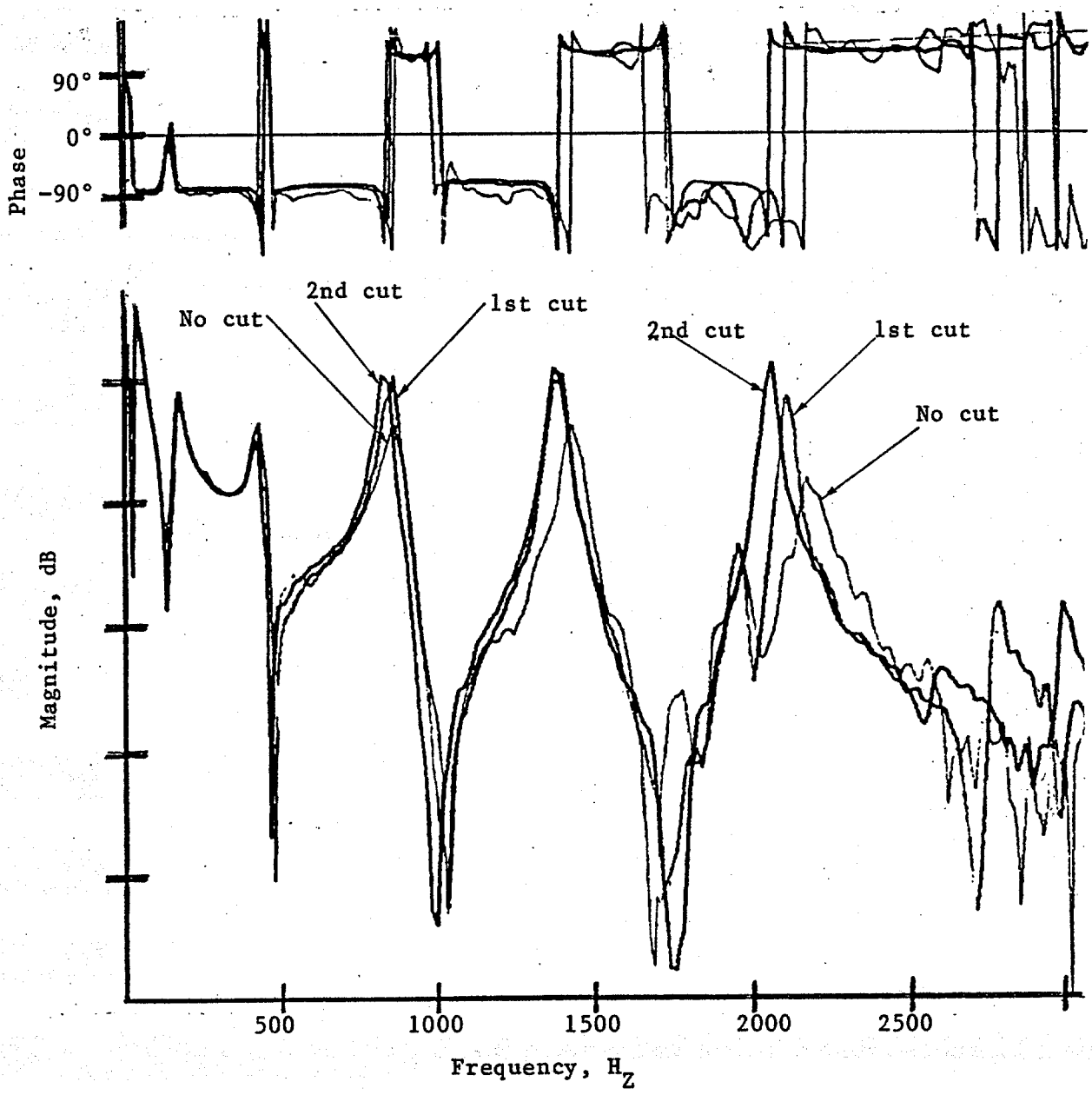

Fig. 21 Transfer Functions at location 6, with force at location 5

the cantilever beam system was simulated with the NASTRAN finite element program.

The input force was an impulse of .4 millisecond duration. The finite element mesh configuration is shown in Fig. 22. Cracks were simulated by opening the grid points along the middle line of accelerometer positions 5 and 6. Three cracks were simulated, each 1/8-inch progressively deeper than the previous one. The natural frequencies of the first six modes for the no-crack and the three-crack scenario were calculated and are shown in Table 9.

Table 9

Natural frequencies of the beam calculated by NASTRAN

Mode No.	No crack	1st crack	2nd crack	3rd crack
1	25.17 Hz	25.10 Hz	24.98 Hz	24.59 Hz
2	157.2	156.73	156.67	156.54
3	439.5	437.45	437.38	435.83
4	861.1	854.50	852.90	853.87
5	1421.0	1405.90	1401.30	1384.80
6	2089.0	2060.60	2055.10	2041.40

When modal damping values were added into the frequency response of the beam, the transfer functions at six accelerometer position was calculated and plotted in Fig. 23-28. The added modal damping ratios corresponding to each mode are listed below, Table 10.

Table 10

Mode No.	Added Modal Damping Ratio
1	12.5 %
2	5.1 %
3	1.25 %
4	0.95 %
5	0.46 %
6	0.175%

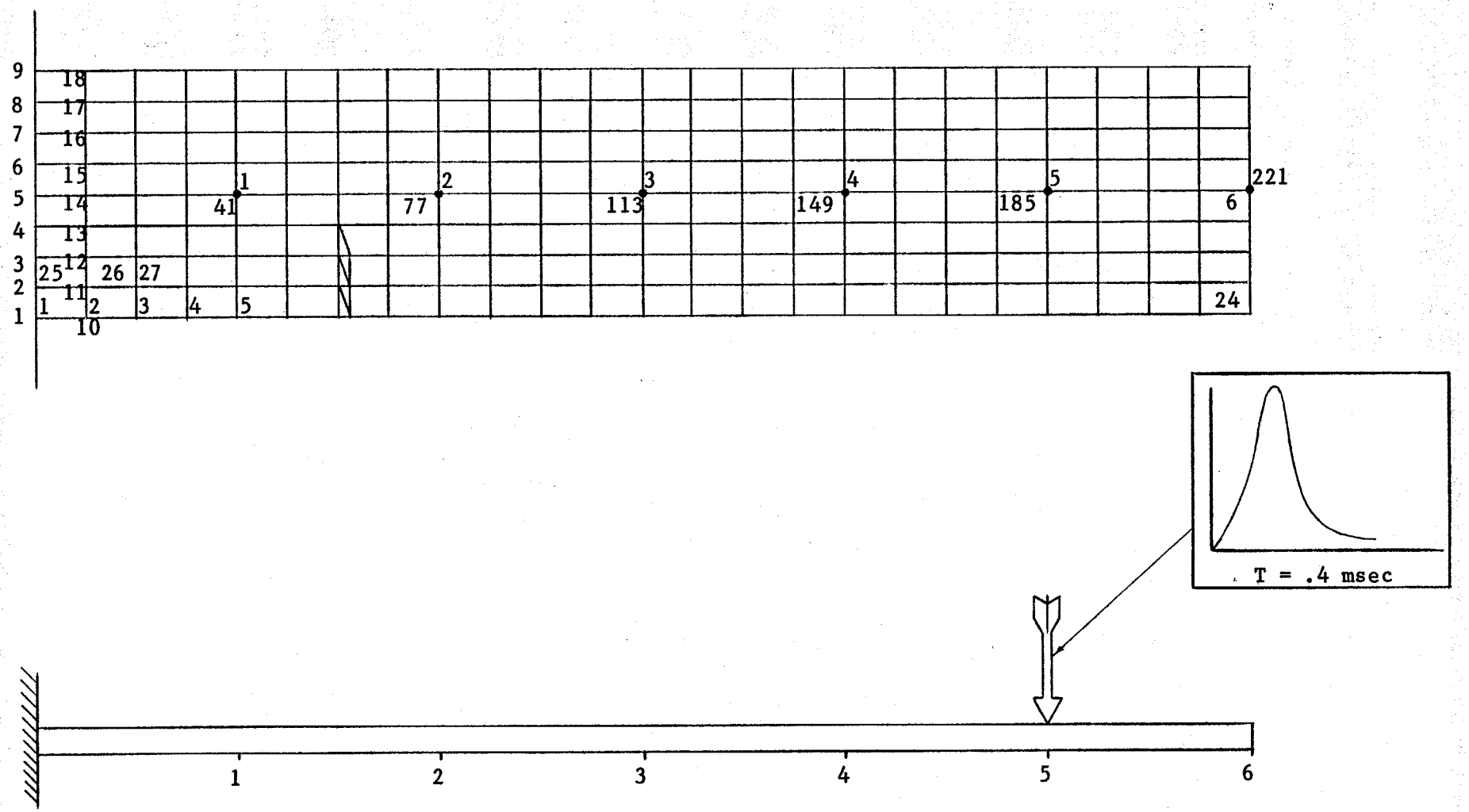

Fig. 22 Finite element mesh configuration used in the NASTRAN simulation

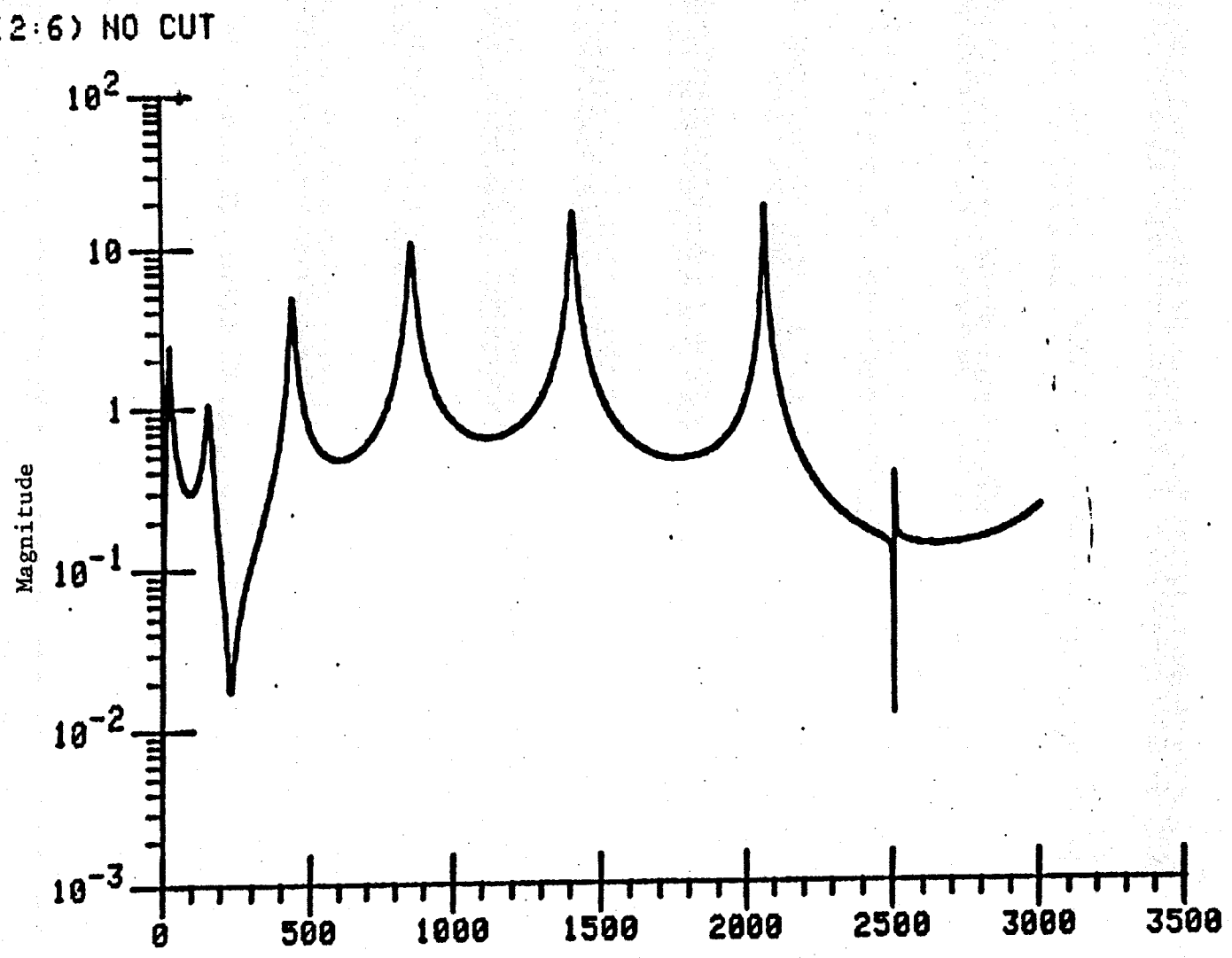

Fig. 23 Simulated Transfer Function at location 1, with force at location 5(No Crack)

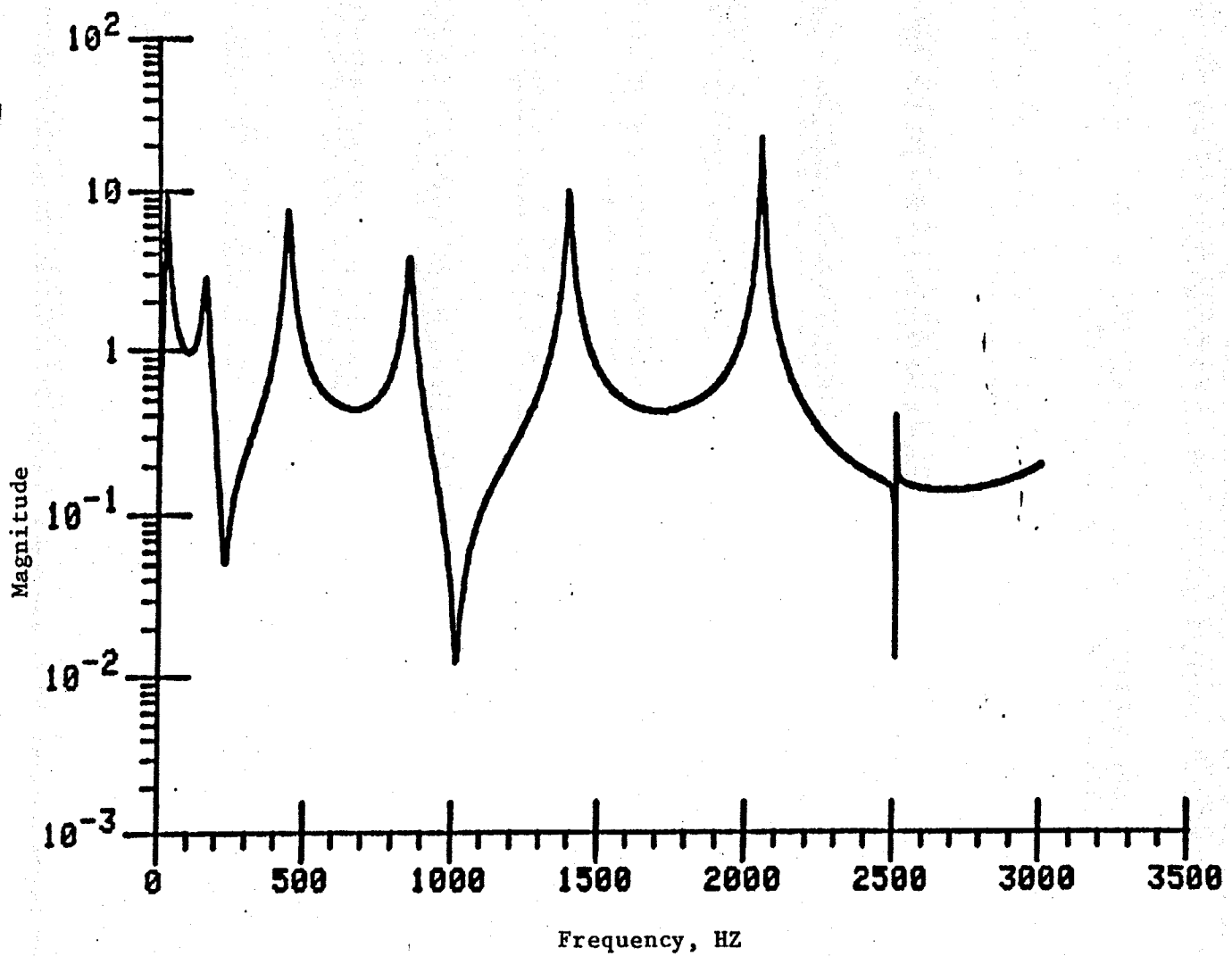

Fig.24 Simulated Transfer Function at location 2, with force at location 5(No Crack)

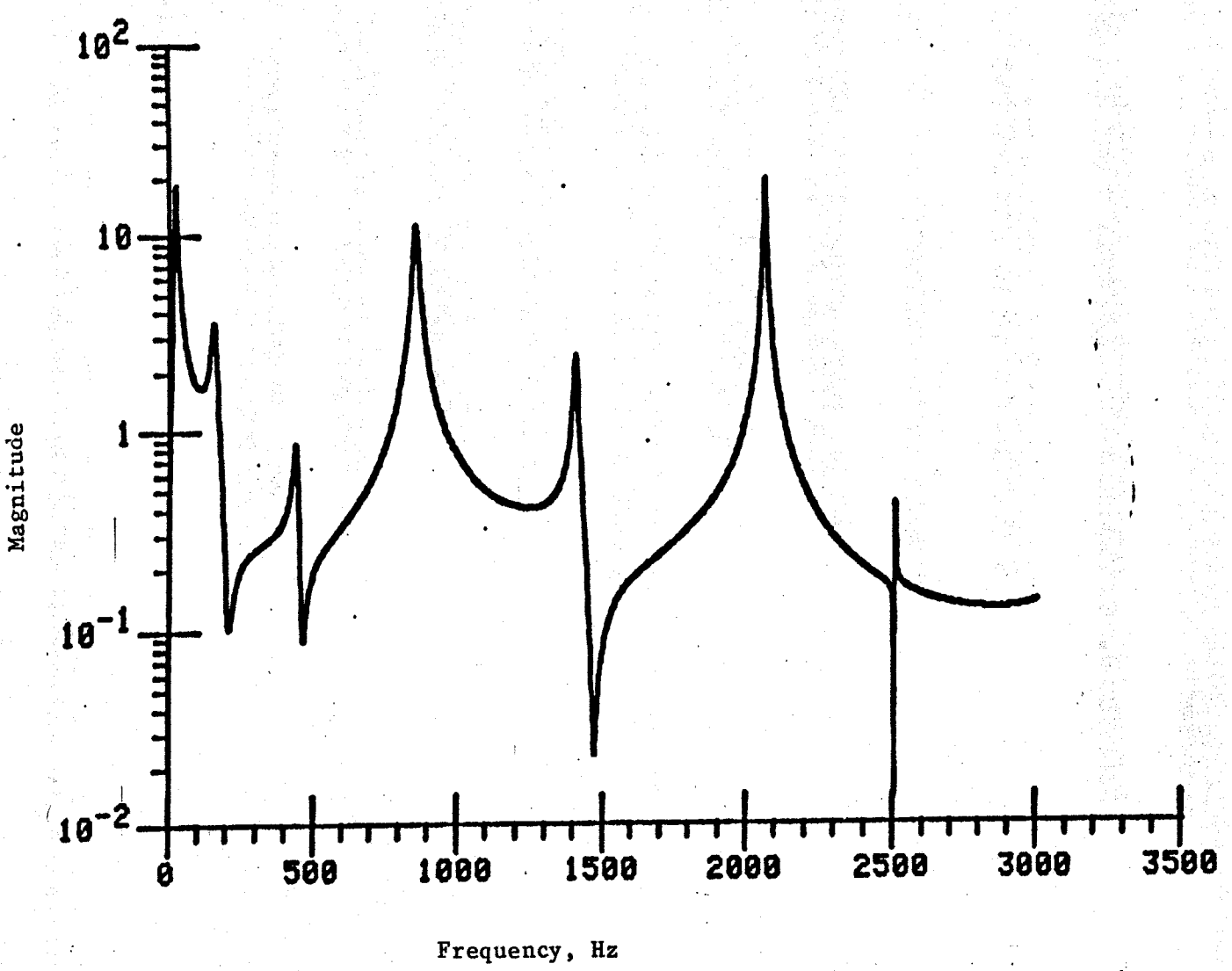

Fig. 25 Simulated Transfer Function at Location 3, with force at location 5 (No crack)

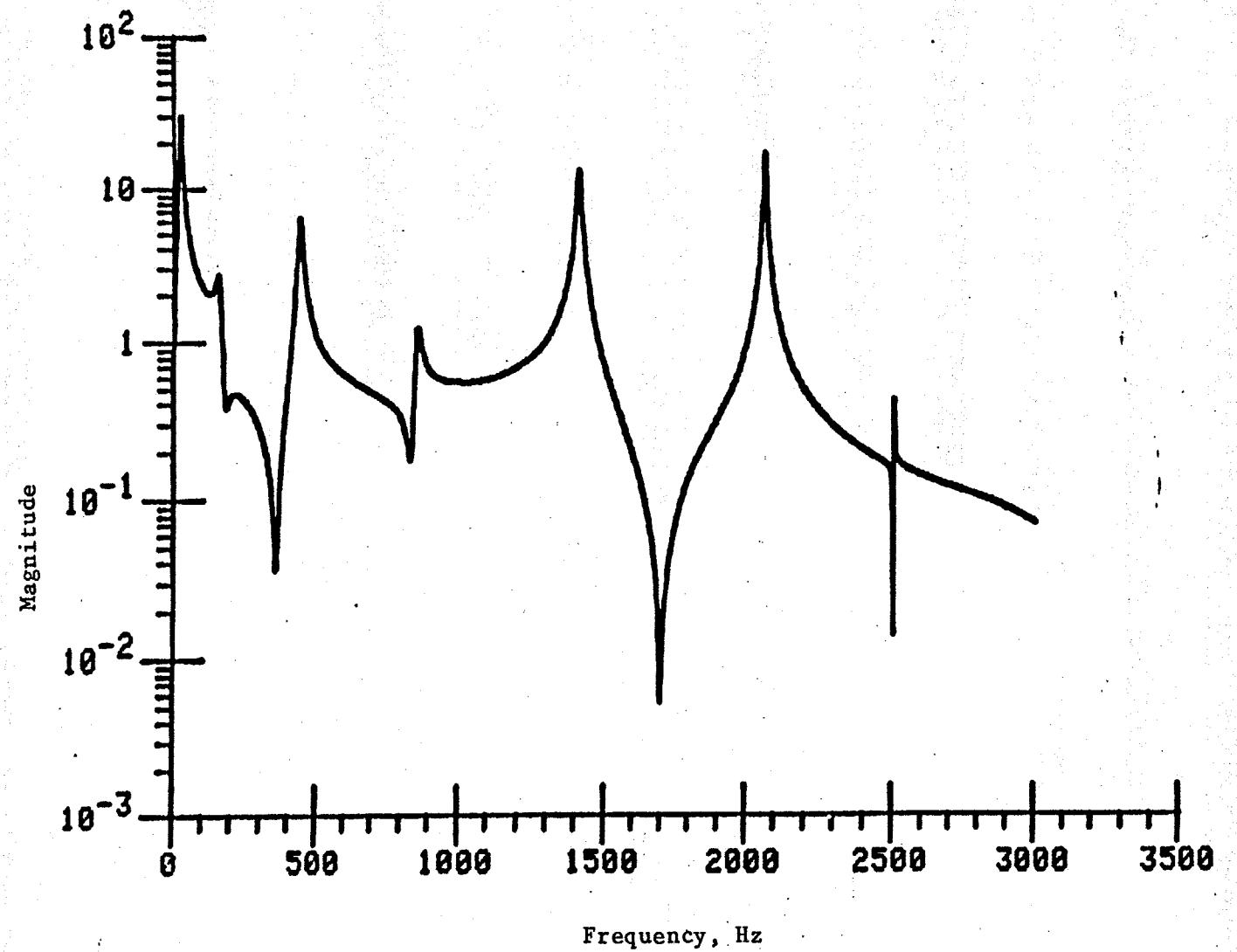

Fig. 26 Simulated Transfer Function at location 4, with force at location 5 (No crack)

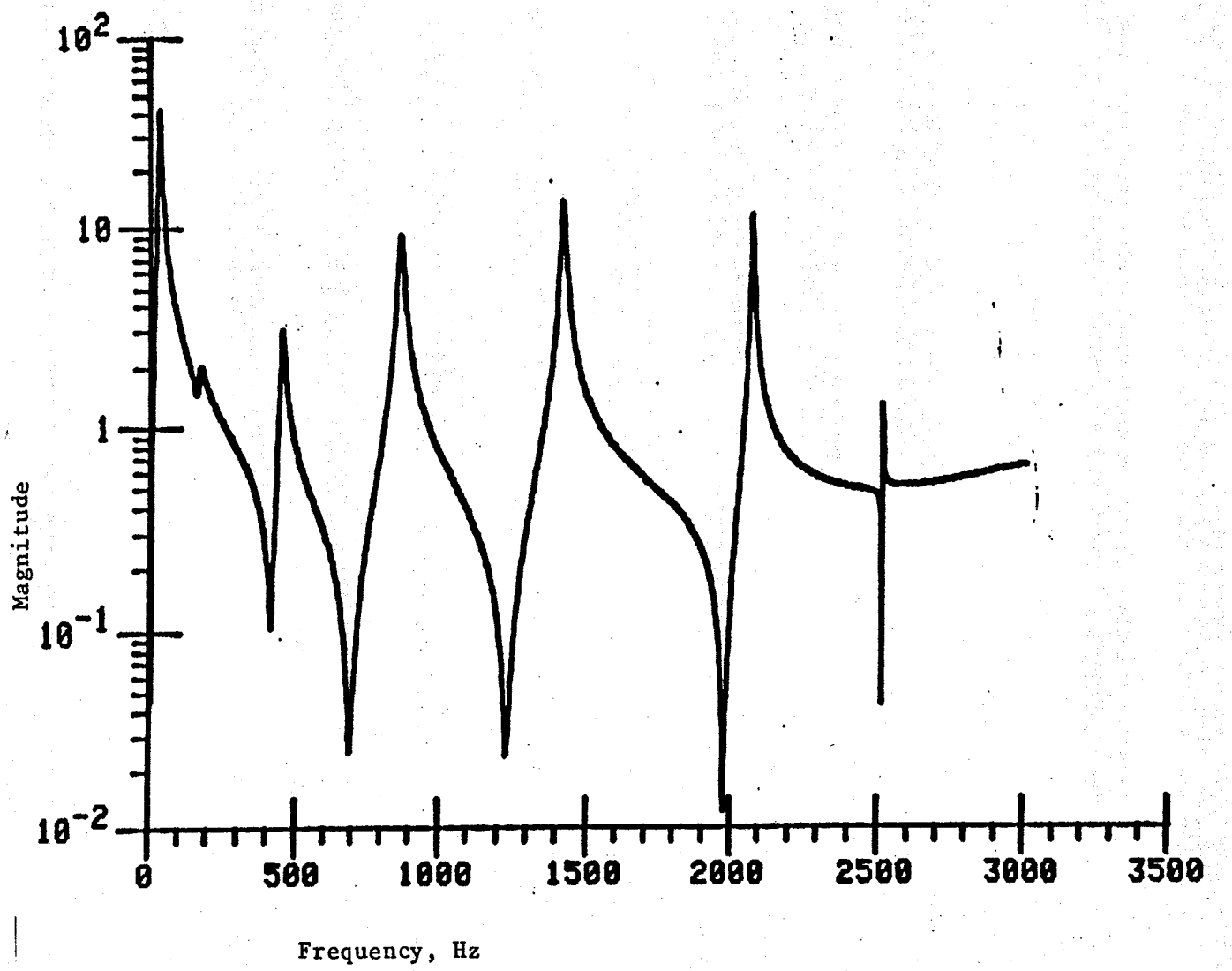

Fig. 27 Simulated Transfer Function at location 5, with force at location 5 (no crack(

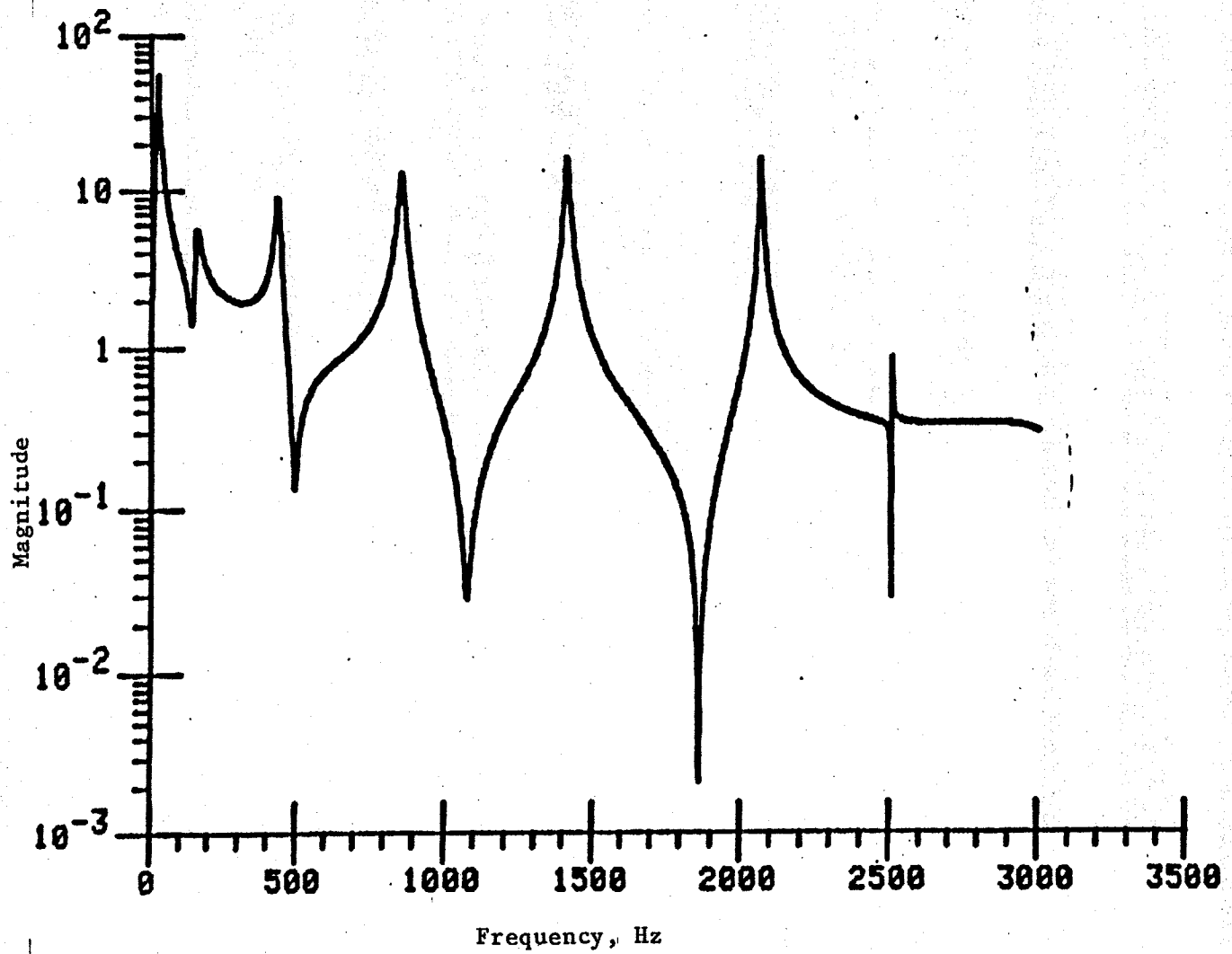

Fig. 28 Simulated Transfer Function at location 6, with force at location 5 (No crack)

In future research these transfer functions will be used as inputs into the frequency domain curve fitting program from which eigenvalues and eigenvectors will be calculated. Then the system's [M][C][K] matrices will be reconstructed from these eigenvalues and eigenvectors using the developed system identification technique. It is expected that the results will show that the crack depth has a detectable effect on the identified system parameters. Future research will deal with correlating crackage and location with observed changes.

8. Conclusions/Recommendations

The feasibility of using structural response data from a known random input to completely characterize the System Parameters, [M][C][K], has been demonstrated for discrete spring-mass-dashpot systems. Both the frequency domain curve fitting and the time domain curve fitting algorithms can give satisfactory eigenvalues and eigenvectors of the system. When the system's parameters are gradually changed the present identification technique is able to resolve the difference and thus show the feasibility of tracking progressive fracture of structural systems.

Preliminary research on a continuous system such as a cantilever beam with induced cracks (saw cuts) and excited by a random imput, indicates that the crack size manifests itself by detectable changes in the transfer function at the higher frequency modes. Analyses of the response data by the System Identification Technique gives promise that the effects of the crack size can be detected by changes in the [M][C][K] matrices. There remains a question of how many degrees of freedom the [M][C][K] matrices should have to represent a

continuous system. When the number of degrees of freedom is large, difficulties will arise concerning the computation accuracy. Therefore the following recommendations are made:

1. Relate the identified [M][C][K] parameters to local physical parameters so that positional information can also be retrieved.
2. Investigate the numerical accuracy and stability when the number of degrees of freedom is high, so that the present system identification technique can be applied to large structural systems.

Appendix I

Random Decrement Analysis Identification Algorithm

The Random Decrement Analysis is a relatively new technique (22-28), it can process the response of a randomly excited system to produce its free response. The free response contains a lot of useful information about the system.

The Random Decrement Technique was originally developed by Mr. H. A. Cole for the measurement of damping and for the detection of structural deterioration or airplane wings subjected to wind flutter excitation (22, 23). Other applications have then been studied by Yang and his graduate students (24-28).

Random Decrement technique is a fast-converging method for extracting meaningful information from random data. It is a process by which segments of the random vibration response of a transducer placed on an object which is subjected to random excitation are ensemble averaged to form a signature which is representative of the free vibration decay curve of the structure. This signature can be used to measure damping or detect incipient failures. The method is particularly useful in field measurements of structures and mechanical systems because excitation is provided naturally by such random inputs as acoustic noise, fluid flow, wing, etc. . . .

In this section we present a brief, rather intuitive explanation of the principles of Random Decrement technique.

The response $x(t)$ of a linear system is governed by the following basic equation:

$$m\,\ddot{x}(t) + c\cdot\dot{x}(t) + k\,x(t) = f(t) \qquad (1)$$

The solution of this differential equation depends on its initial conditions and the excitation $f(t)$. Since, for linear systems the superposition law applies, the response can be decomposed into three parts: response due to initial displacement $x_d(t)$, response due to initial velocity $x_v(t)$ and finally the response due to the forcing function $x_f(t)$.

The Random Decrement analysis consists of averaging N segments of the length τ_1 of the system response in the following manner: the starting time t_i of each segment is selected such that $x_i(t_i) = x_s$ = constant and the slope $\dot{x}_i(t_i)$ is alternating positive and negative. This process can be represented in mathematical form:

$$\delta(\tau) = \frac{1}{N}\sum_{i=1} x_i(t_i+\tau) \qquad (2)$$

where

$$x_i(t_i) = x_s \qquad i = 1, 2, 3 \ldots$$

$$\dot{x}_i(t_i) = \geq 0 \qquad i = 1, 3, 5 \ldots$$

$$\dot{x}_i(t_i) = \leq 0 \qquad i = 2, 4, 6 \ldots$$

The function $\delta(\tau)$ is called the Random Decrement signature and is only defined in the time interval $0 \leq \tau \leq \tau_1$. The meaning of the Random Decrement signature can now be determined. If the parts due to initial velocity are averaged together, they cancel out because alternately parts with positive and negative initial slopes are taken and their distribution is random. Furthermore, if the parts due to the excitation are averaged they also vanish because, by definition, the excitation is random. Finally only the parts due to initial displacement are left and their average is the Random Decrement signature representing the free vibration decay curve of the system due to an initial displacement, which corresponds to the bias level x_s. (Fig. 1)

In reality the Randomdec computer converts each segment into digital form and adds it to the previous segments (Fig. 2); the average is then stored in the memory and can be displayed on a screen. The number of segments to be averaged for the Random Decrement signature depends on the signal shape, usually 400 to 500 averages are sufficient to produce a repeatable signature.

One particularly interesting characteristic of Randomdec technique should be mentioned: it requires no knowledge of the excitation f(t) as long as it is random. Neither the type not the intensity of the input affect the signature.

For a single-degree-of-freedom system the natural frequency and damping ratio can be calculated directly from the Random Decrement Signature by the logarithmic decrement measurement since the signature is a free vibration decay curve of the system. For multi-degree-of-freedom systems where the modes are well separated these can be determined by bandpass filtering the response data about the natural frequency first to yield a single-mode Random Decrement Signature of interest. However, if the principle modes of a multi-degree-of-freedom system are closely spaced, they cannot be separated by a filter without distorting the Random Decrement Signature. In such a case curve fitting is introduced to solve this problem. This curve fitting program uses an optimization algorithm which finds the best combination of natural frequencies and damping ratios that minimizes the mean square error between a mathematical function, which describes the response, and the Random Decrement data.

We plan to use the Random Decrement produced free response of a system to obtain its eigenvalues. This should be a more accurate way to find the eigenvalues of systems with high modal density than the standard frequency response half power point method.

A special optimization curve fitting program will be developed for this purpose. The mathematical expression of the free response of linear

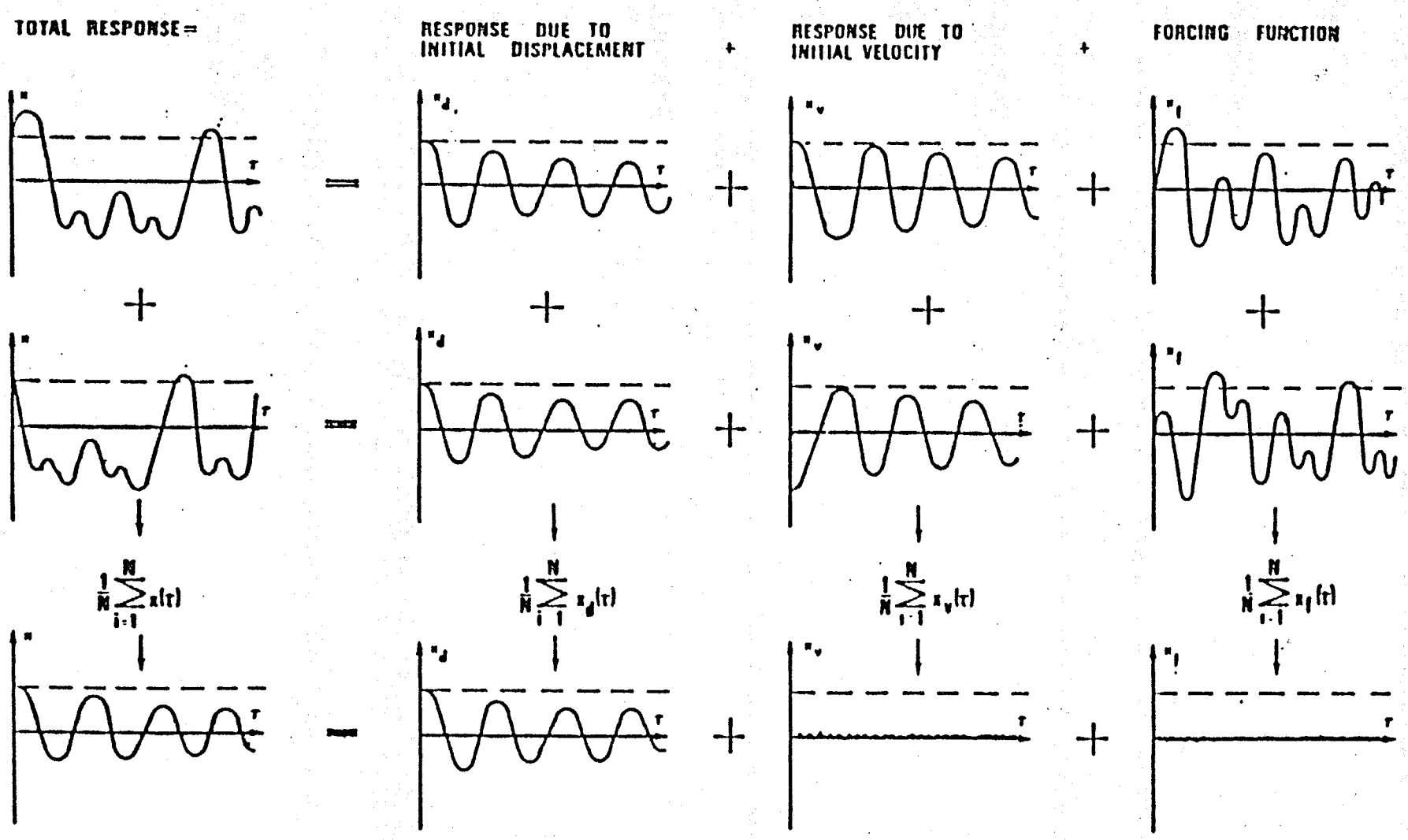

Figure 1: Principles of Randomdec Technique.

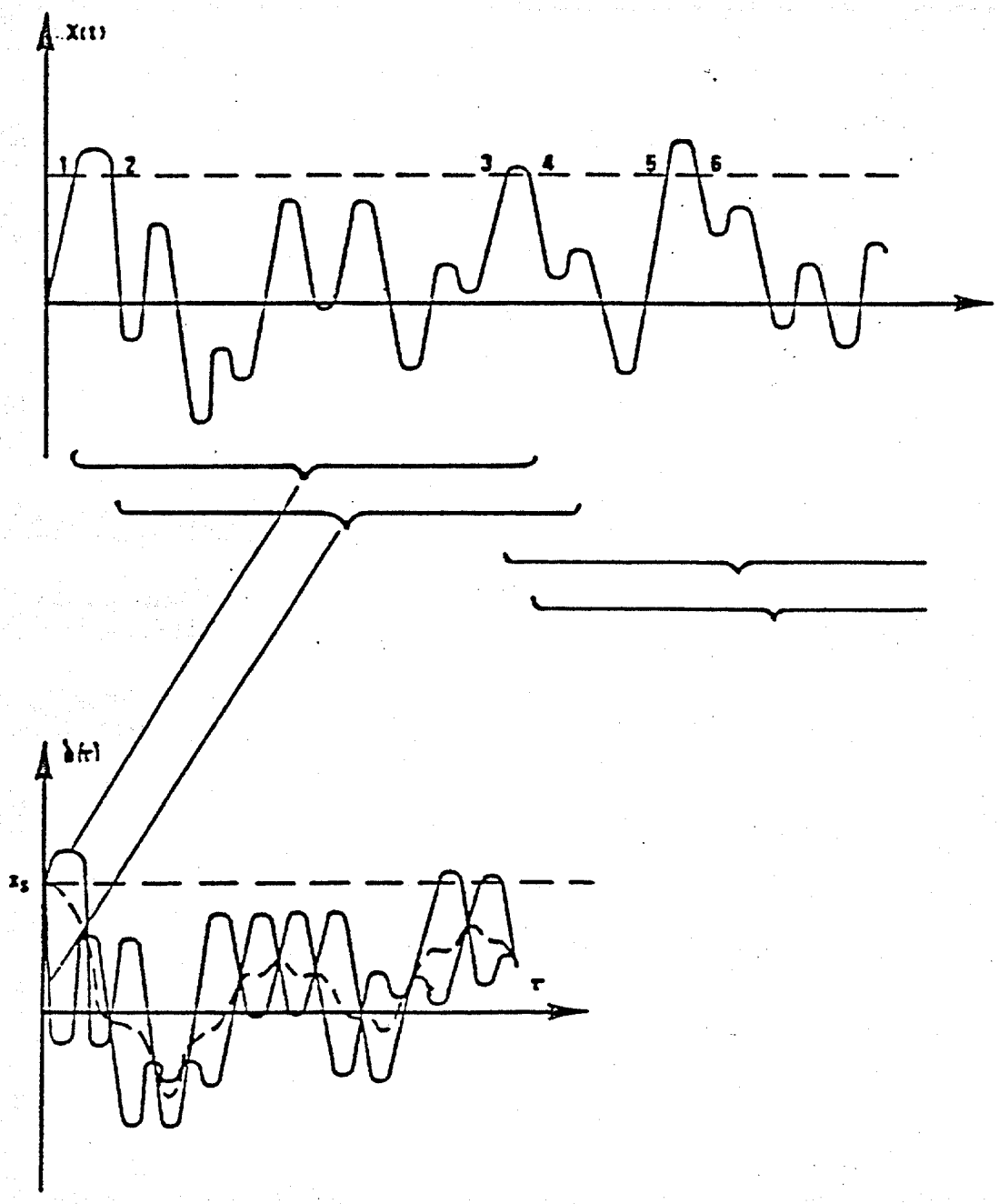

Figure 2: Extraction of the Randomdec signature.

dynamic systems is given by equation (3)

$$x_i(t) = \alpha_o + \sum_{i=1}^{W_2} \alpha_i \, e^{-\omega_i \zeta_i t} \sin(w_i t + \phi_i) \qquad (3)$$

where ω_i and ζ_i are the unknown natural frequency and damping ratio of the ith mode of the system. The objective of the Random Decrement curve fitting program then will be to obtain the proper values of these unknown so that equation (3) accurately describes the experimental response data.

Appendix II Frequency Domain Curve Fitting Method

1. INTRODUCTION

In 1959, Levy [29] presented a method for estimating the coefficients of a rational transfer function expression of a linear system from the measured frequency response. He suggested the use of the denominator as the weighting on the estimation error and formulated a linear least square approach to the problem. The drawback of this is that the emphasis on higher frequency values causes unsatisfactory fit at low frequencies. Sanathanan and Koerner [30] improved Levy's method with an iteration procedure which effectively eliminates the unfavorable weighting factors introduced into the cost function. Based on the results of [29] and [30], Lawrence and Rogers [31] presented a recursive algorithm to solve this problem while Jong and Shanmugam [32] presented a method fitting only the amplitude of the frequency response data. They used the iteration procedures similar to what Sanathanan, et al. used in [30] to remove the unwanted weighting factors. With this approach all data values are weighted evenly and the fit is good in both the lower and higher frequency ends. But difficulty can still be encountered. A transfer function when expressed in partial fraction form can be characterized by its poles and the associated residues. If the ratio of the residues corresponding to two poles of the system is substantial, the method used in [30], [31] and [32] may fail. In this event, the pole with the small residue can disappear from the identified eigenvalue table. In order to overcome this problem, a set of new weighting factors is introduced into the original cost function by iteration, such that the new cost function to be minimized is the sum of the squared "relative" errors.

2. THEORETICAL DEVELOPMENT

The relation between the ideal and the measured frequency response of a system can be expressed in the following equation

$$g(j\omega) - z(j\omega) = \varepsilon(j\omega) \tag{1}$$

where $z(j\omega)$ is the measured data, $\varepsilon(j\omega)$ is the measurement noise and $g(j\omega)$ is the ideal frequency response. If the system is linear, it is common to assume that the transfer function can be written as

$$g(j\omega) = \frac{a_1+a_2(j\omega)+\ldots+a_{n+1}(j\omega)^n}{b_1+b_2(j\omega)+\ldots+b_m(j\omega)^{m-1}+(j\omega)^m} = \frac{n(j\omega)}{d(j\omega)} \tag{2}$$

Given a set of measurements, $z(j\omega_k) = \alpha_k + j\beta_k$, $(k = 1,2,\ldots,s)$, and assuming that n and m are known $(n \leq m)$, the problem of interest here is to estimate coefficients a_i and b_i in (2) by minimizing some cost function of $\varepsilon(j\omega_k)$. Combining Eqs. (1) and (2), one can obtain

$$n(j\omega_k) - [\alpha_k + j\beta_k]\cdot d(j\omega_k) = \varepsilon(j\omega_k)\cdot d(j\omega_k) \quad (k=1,2,\ldots,s) \qquad (3)$$

With the definition of the following

$$x = [a_1\ a_2\ \cdots\ a_{n+1}\ b_1\ b_2\ \cdots\ b_m]^T$$

$$p_k = [(j\omega_k)^0\ (j\omega_k)^1\ (j\omega_k)^2\ \cdots\ (j\omega_k)^n]^T = p_{kR} + jp_{kI}$$

$$q_k = [(j\omega_k)^0\ (j\omega_k)^1\ (j\omega_k)^2\ \cdots\ (j\omega_k)^{m-1}]^T = q_{kR} + jq_{kI}$$

Eq. (3) can be conveniently rewritten in a matrix form as

$$A_k x - y_k = e_k \quad (k=1,2,\ldots,s) \qquad (4)$$

where

$$A_k = \left[\begin{array}{c|c} p_{kR}^T & -\alpha_k q_{kR}^T + \beta_k q_{kI}^T \\ \hline p_{kI}^T & -\alpha_k q_{kI}^T - \beta_k q_{kR}^T \end{array}\right]_{2x(m+n+1)}$$

$$y_k = \left[\begin{array}{c} \mathrm{Re}[(\alpha_k+j\beta_k)\cdot(j)^m] \\ \mathrm{Im}[(\alpha_k+j\beta_k)\cdot(j)^m] \end{array}\right]_{2x1} \cdot \omega_k^m$$

$$e_k = \left[\begin{array}{c} \mathrm{Re}[\varepsilon(j\omega_k)\cdot d(j\omega_k)] \\ \mathrm{Im}[\varepsilon(j\omega_k)\cdot d(j\omega_k)] \end{array}\right]_{2x1}$$

Eq. (4) can be further condensed and written as

$$Ax - y = e \qquad (5)$$

where

$$A = [A_1^T\ A_2^T\ \ldots\ A_k^T\ \ldots\ A_s^T]^T$$

$$y = [y_1^T\ y_2^T\ \ldots\ y_k^T\ \ldots\ y_s^T]^T$$

$$e = [e_1^T\ e_2^T\ \ldots\ e_k^T\ \ldots\ e_s^T]^T$$

With least-square approach one can find the best estimate of x for Eq. (5) that minimizes the following cost function

$$E_o = ||e||^2 = \sum_{k=1}^{s} |\varepsilon(j\omega_k)d(j\omega_k)|^2 \qquad (6)$$

is

$$x = (A^TA)^{-1}A^Ty \qquad (7)$$

This is, in fact, the same result as what Levy got in [2].

Instead of eliminating the weighting factors, $d(j\omega_k)$ in Eq. (6) as what others do [3-5], a new set of weighting factors is introducted here into Eq. (6) through iterations. The procedure is as follows.

1. Let $n(j\omega_k)_L$ and $d(j\omega_k)_L$ be the values of $n(j\omega_k)$ and $d(j\omega_k)$, respectively, based on the estimate of x in the L-th iteration.

2. Replace $n(j\omega_k)$ and $d(j\omega_k)$ with $n(j\omega_k)_L$ and $d(j\omega_k)_L$, respectively, in Eq. (3) and divide both sides by $n(j\omega_k)_{L-1}$ to yield

$$\frac{n(j\omega_k)_L - z(j\omega_k)d(j\omega_k)_L}{|n(j\omega_k)_{L-1}|} = \frac{\varepsilon(j\omega_k)d(j\omega_k)_L}{|n(j\omega_k)_{L-1}|} \qquad (8)$$

3. Rewrite eqn. (8) in matrix form as

$$D_kA_kx_L - D_ky_k = D_ke_k \quad (k=1,2,\ldots,s) \qquad (9)$$

where

$$D_k = \frac{1}{|n(j\omega_k)_{L-1}|} \begin{bmatrix} 1 & 0 \\ 0 & 1 \end{bmatrix} \quad (k=1,2,\ldots,s)$$

4. Combine all equations in Eq. (9) together in the following matrix equation,

$$DAx_L - Dy = De \qquad (10)$$

where

$$D = \begin{bmatrix} D_1 & & & 0 \\ & \ddots & & \\ & & D_k & \\ & & & \ddots \\ 0 & & & D_s \end{bmatrix}$$

5. Formulate the new cost function as

$$E_1 = ||De||^2 = \sum_{k=1}^{s} |\epsilon(j\omega_k) d(j\omega_k)_L / n(j\omega_k)_{L-1}|^2 \qquad (11)$$

6. Obtain the best estimate of x_L for the L-th iteration

$$x_L = (A^T Q A)^{-1} A^T Q y \qquad (12)$$

where $Q = D^T D = D^2$

To initiate the procedure, or equivalently for L = 1, one can assume $|n(j\omega_k)_o| = 1$, which will give Levy's result of a_i's as the result of the first iteration.

3. EXAMPLE

A numerically generated example is described in the following.

An 8th order system with system coefficients given in Table 1 is used to test the algorithm. Also included in Table 1 are the poles and residues associated with the partial fraction expression of the system transfer function, and the damping ratio associated with the complex poles. Frequency response data are numerically generated according to Eq. (2) with the system coefficients in Table 1. The resulted real and imaginary parts of this set of data are plotted and shown in Fig. 1. Alternatively, the magnitude and phase angle can be obtained, and they are displayed in Fig. 2.

The system coefficients determined with the new algorithm on the generated data are listed in Table 2 which also includes residues, poles and dampings. The frequency response data generated with the fitted coefficients are shown in Figs. 3 and 4. Evenly weighted algorithm which was introduced by Sanathanan and Koerner [30] is also applied to fit the data. The system coefficients so identified are listed in Table 3 while the corresponding response data can be seen in Figs. 5 and 6.

The frequency response data are free from any noises other than the numerical truncation errors. It is quite obvious from Tables 1, 2 and 3 that with the new algorithm the identified system coefficients are almost identical to the exact ones while with the other algorithm the coefficients are completely different. The substantial difference between the coefficient sets, however, does not cause the frequency response curves to be drastically different as can be seen in Figs. 3 and 5 or in Figs. 4 and 6. Both frequency responses are very similar to the exact ones that are shown in Figs. 1 and 2. The poles of the system are all complex conjugates and the ones identified with the new algorithm are almost identical to them as can be learned from Tables 1 and 2. In the same tables, one can also see that the residues are very similar for all the poles. In Table 3, it can be seen that the poles identified with the other algorithm are different than those in Tables 1 and 2. The major distinction between the two identified curves is the feature around 400 rad/sec as can be seen from comparing Figs. 1, 3 and 5. The more pronounced difference is easily spotted in the phase angle curves shown in Figs. 2, 4 and 6. The poles not found with Sanathanan and Loerner's algorithm are the third complex conjugate pair of which the imaginary part is 406.7. This number corresponds to the frequency in rad/sec around which the distinction between the identified curves is most prominent.

COEFFICIENTS OF NUMERATOR:

A(1)= -.1684+17	A(2)= -.4844+14	A(3)= -.1641+14
A(4)= -.5412+10	A(5)= -.1871+09	A(6)= -.3842+05
A(7)= -.5232+03	A(8)= -.6298-01	

COEFFICIENTS OF DENOMINATOR:

B(1)= .3227+19	B(2)= .1008+17	B(3)= .3540+16
B(4)= .1287+13	B(5)= .1556+12	B(6)= .1447+08

RESIDUES:	POLES:	DAMPING:
.1097-03 .7020-02	-.1367+01 .3082+02	.4430-01
.1097-03 -.7020-02	-.1367+01 -.3082+02	.4430-01
-.1419-01 .3411+00	-.2647+01 .1616+03	.1638-01
-.1419-01 -.3411+00	-.2647+01 -.1616+03	.1638-01
.2352-02 .4493-02	-.3087+01 .4067+03	.7591-02
.2352-02 -.4493-02	-.3087+01 -.4067+03	.7591-02
-.1976-01 .2301+00	-.4554+01 .8858+03	.5141-02
-.1976-01 -.2301+00	-.4554+01 -.8858+03	.5141-02

Table 1. Exact System Coefficients

COEFFICIENTS OF NUMERATOR:

A(1)= -.1688+17	A(2)= -.4829+14	A(3)= -.1645+14
A(4)= -.5365+10	A(5)= -.1875+09	A(6)= -.3837+05
A(7)= -.5242+03	A(8)= -.6440-01	

COEFFICIENTS OF DENOMINATOR:

B(1)= .3229+19	B(2)= .1009+17	B(3)= .3540+16
B(4)= .1282+13	B(5)= .1556+12	B(6)= .1447+08
B(7)= .9774+06	B(8)= .2335+02	

.1502-03 .7001-02	-.1368+01 .3083+02	.4434-01
.1502-03 -.7001-02	-.1368+01 -.3083+02	.4434-01
-.1401-01 .3419+00	-.2624+01 .1616+03	.1623-01
-.1401-01 -.3419+00	-.2624+01 -.1616+03	.1623-01
.2352-02 .4489-02	-.3104+01 .4067+03	.7633-02
.2352-02 -.4489-02	-.3104+01 -.4067+03	.7633-02
-.2069-01 .2305+00	-.4578+01 .8858+03	.5168-02
-.2069-01 -.2305+00	-.4578+01 -.8858+03	.5168-02

Table 2. Identified System Coefficients-New Algorithm

COEFFICIENTS OF NUMERATOR:

A(1)= -.2683+16	A(2)= -.7861+13	A(3)= -.2704+13
A(4)= -.1154+10	A(5)= -.1121+09	A(6)= -.3126+05
A(7)= -.5203+03	A(8)= -.6997-01	

COEFFICIENTS OF DENOMINATOR:

B(1)= .5154+18	B(2)= .1617+16	B(3)= .5825+15
B(4)= .2564+12	B(5)= .4277+11	B(6)= .7870+07
B(7)= .8384+06	B(8)= .1815+02	

.4485-04 .6993-02	-.1371+01 .3080+02	.4448-01
.4485-04 -.6993-02	-.1371+01 -.3080+02	.4448-01
.8224-03 .1357-02	-.4770+00 .1626+03	.2933-02
.8224-03 -.1357-02	-.4770+00 -.1626+03	.2933-02
-.1563-01 .3405+00	-.2653+01 .1616+03	.1641-01
-.1563-01 -.3405+00	-.2653+01 -.1616+03	.1641-01
-.2022-01 .2305+00	-.4576+01 .8858+03	.5165-02
-.2022-01 -.2305+00	-.4576+01 -.8858+03	.5165-02

Table 3. Identified System Coefficients - Sanathanan and Koerner Algorithm

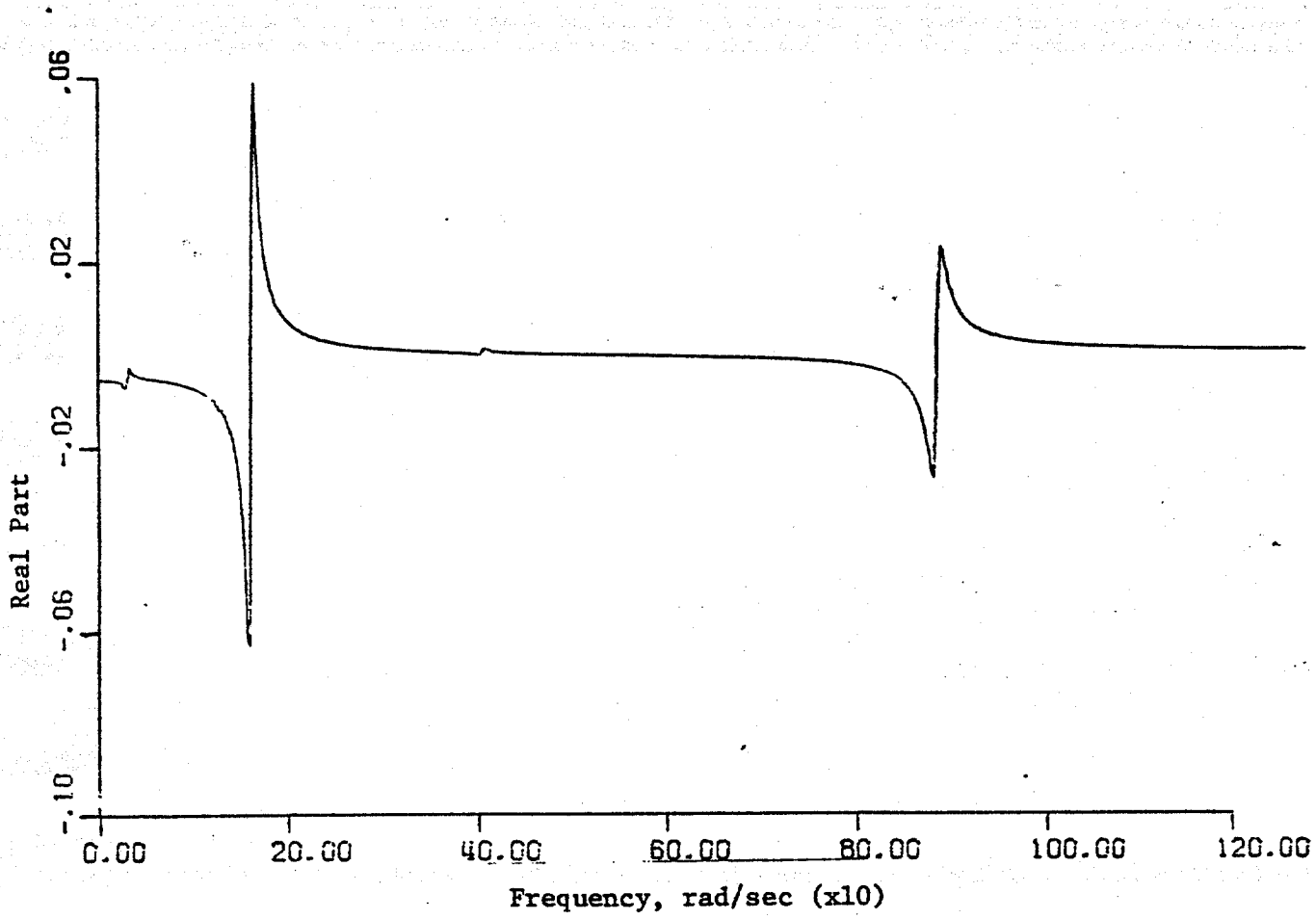

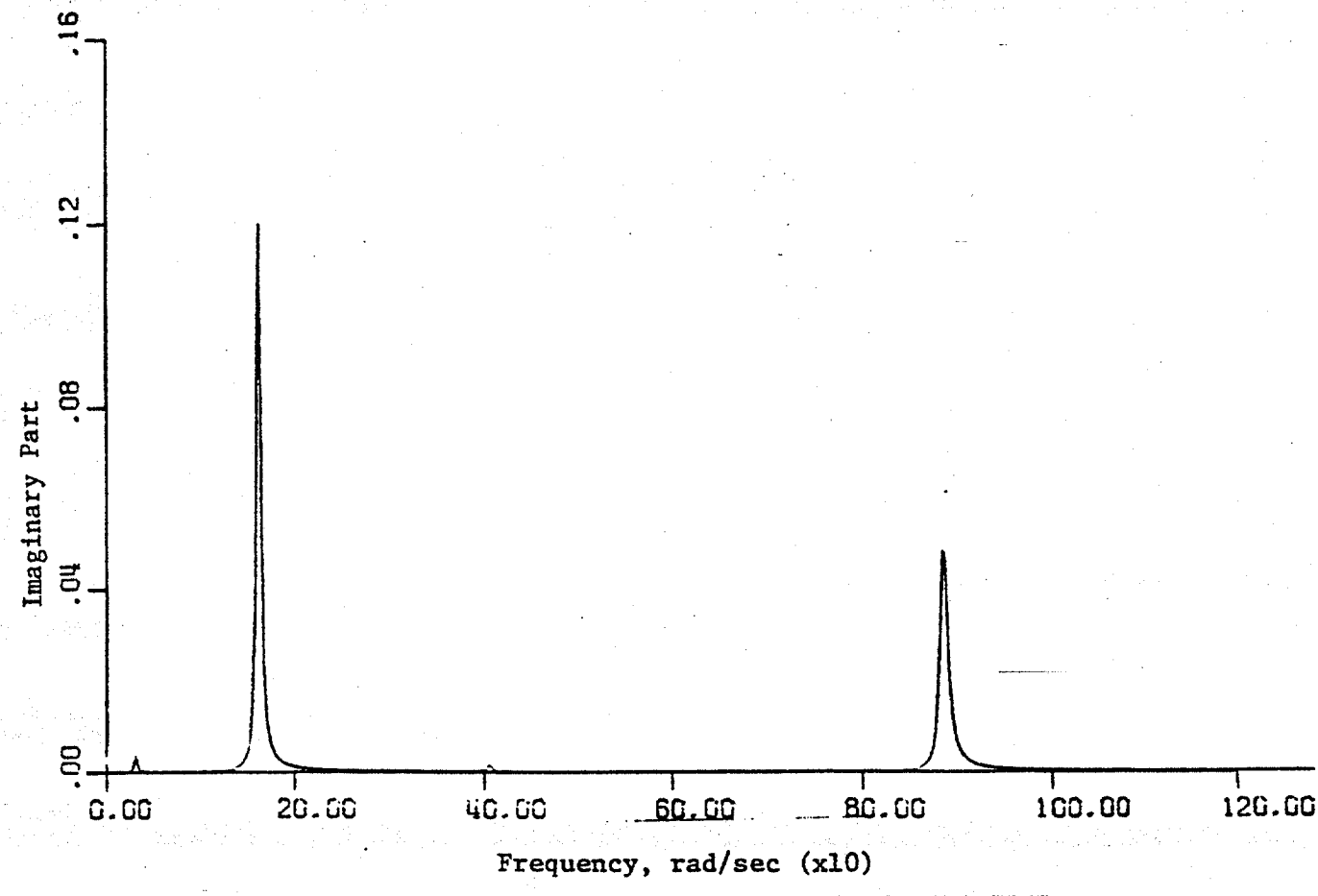

Fig. 1 Frequency Response, Real and Imaginary

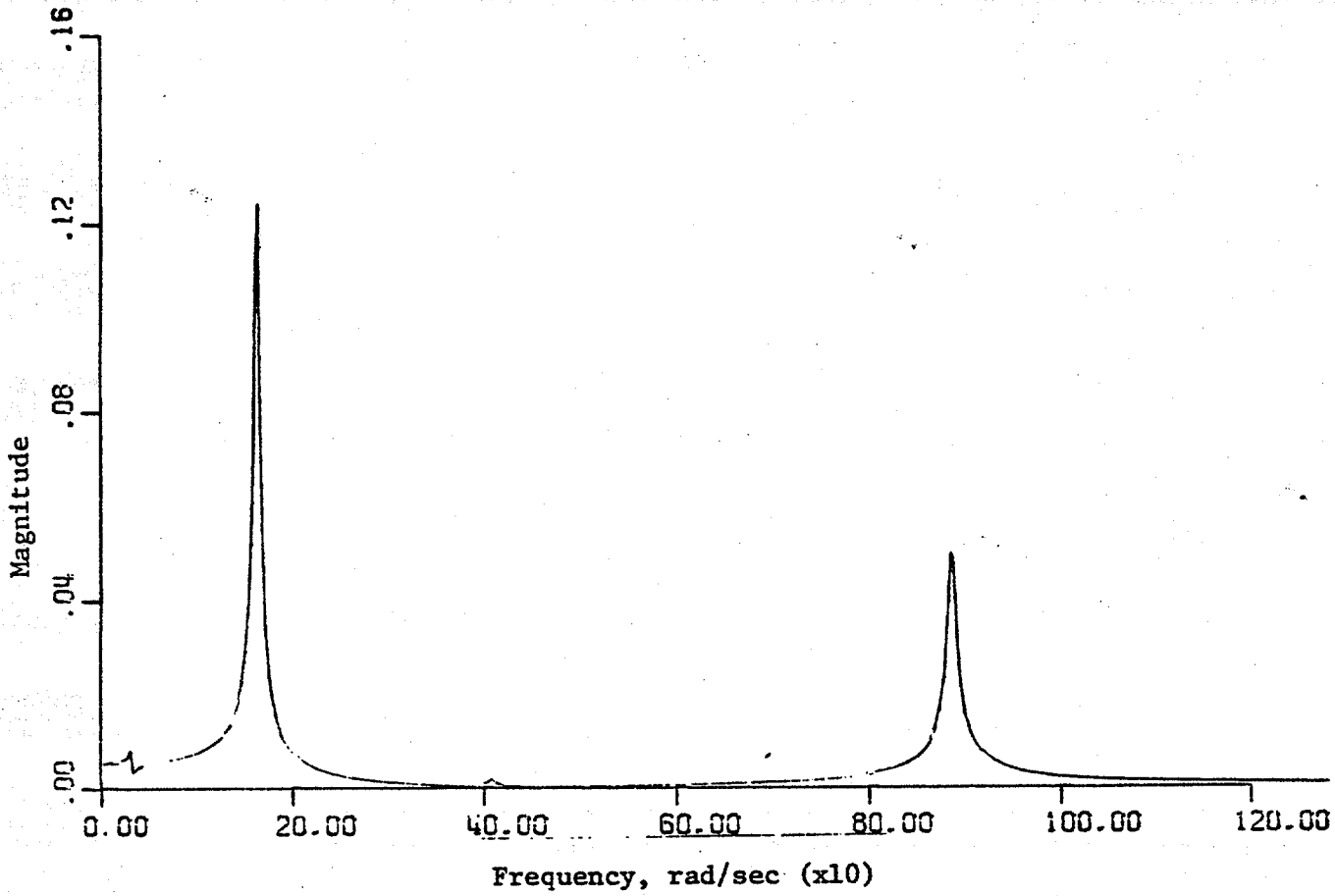

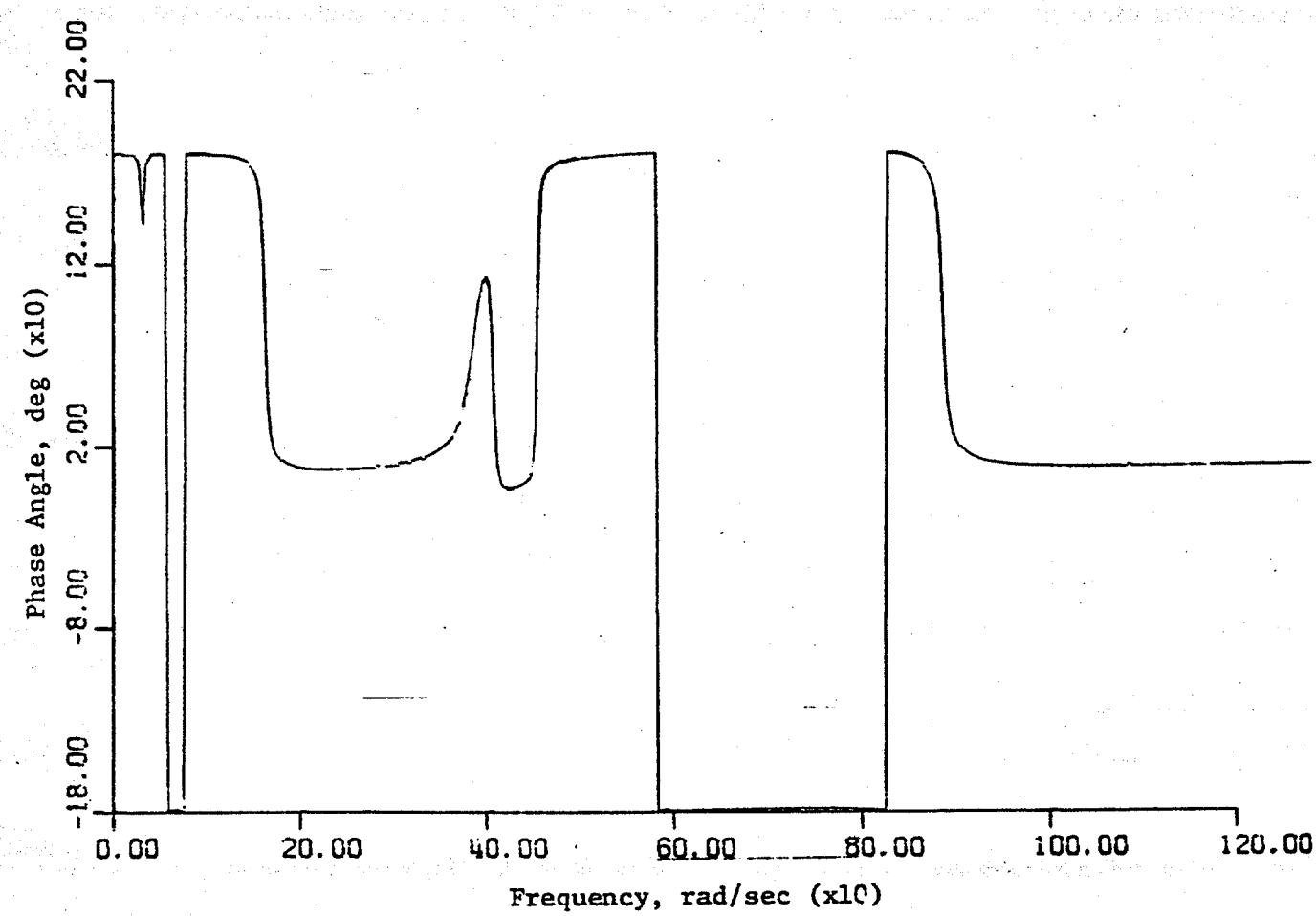

Fig. 2 Frequency Response, Magnitude and Phase Angle

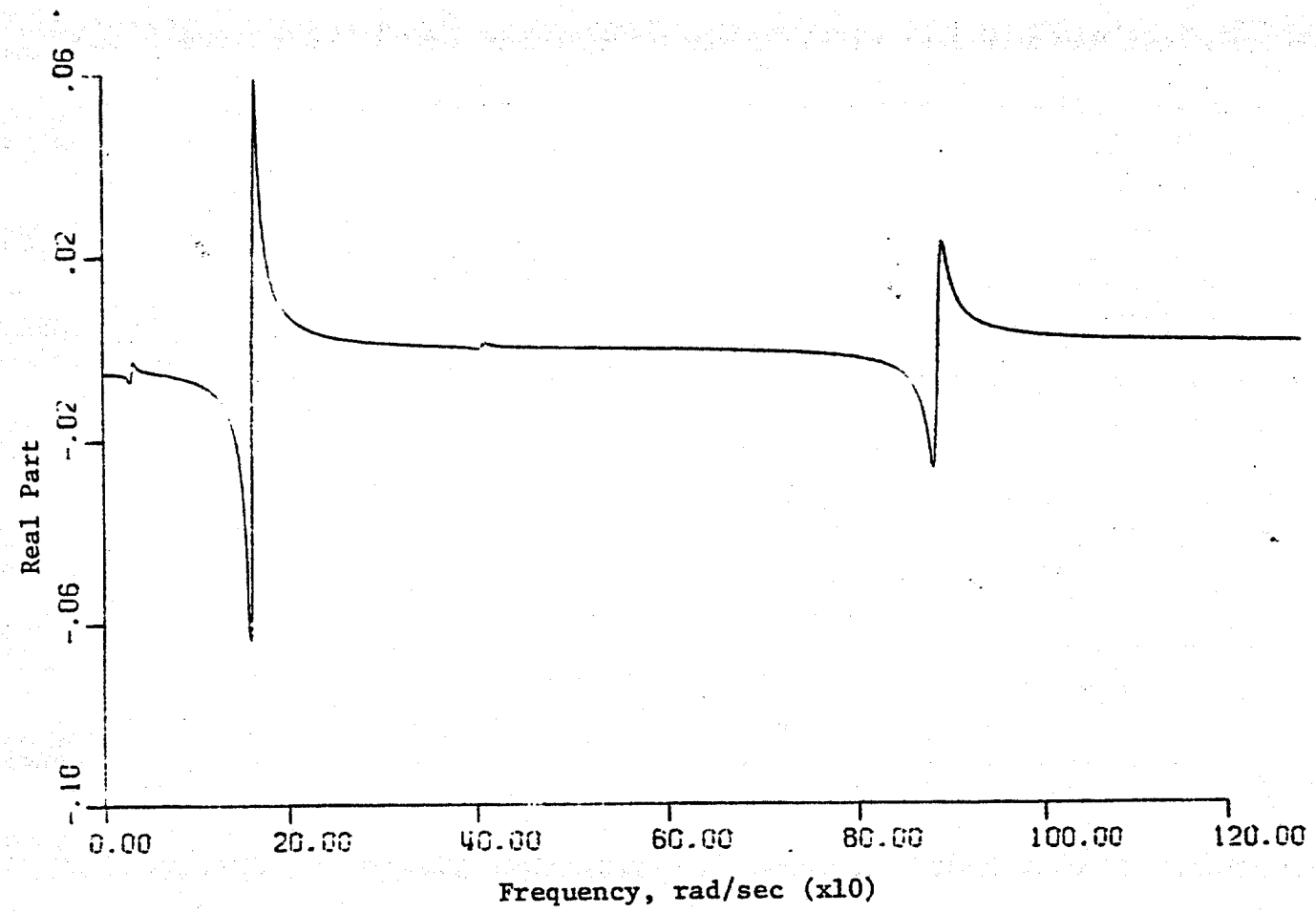

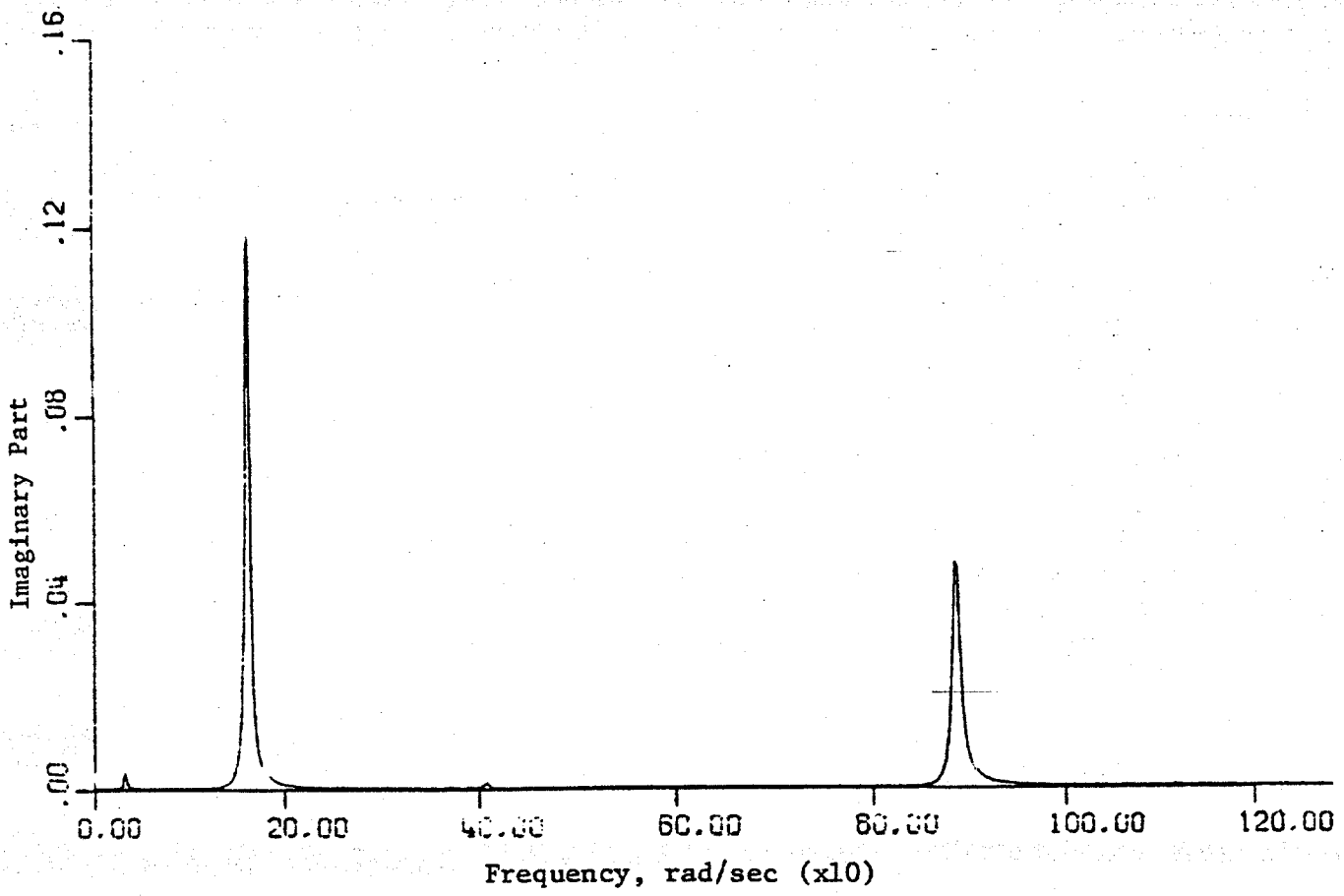

Fig. 3 Fitted Frequency Response, Real and Imaginary, with New Algorithm

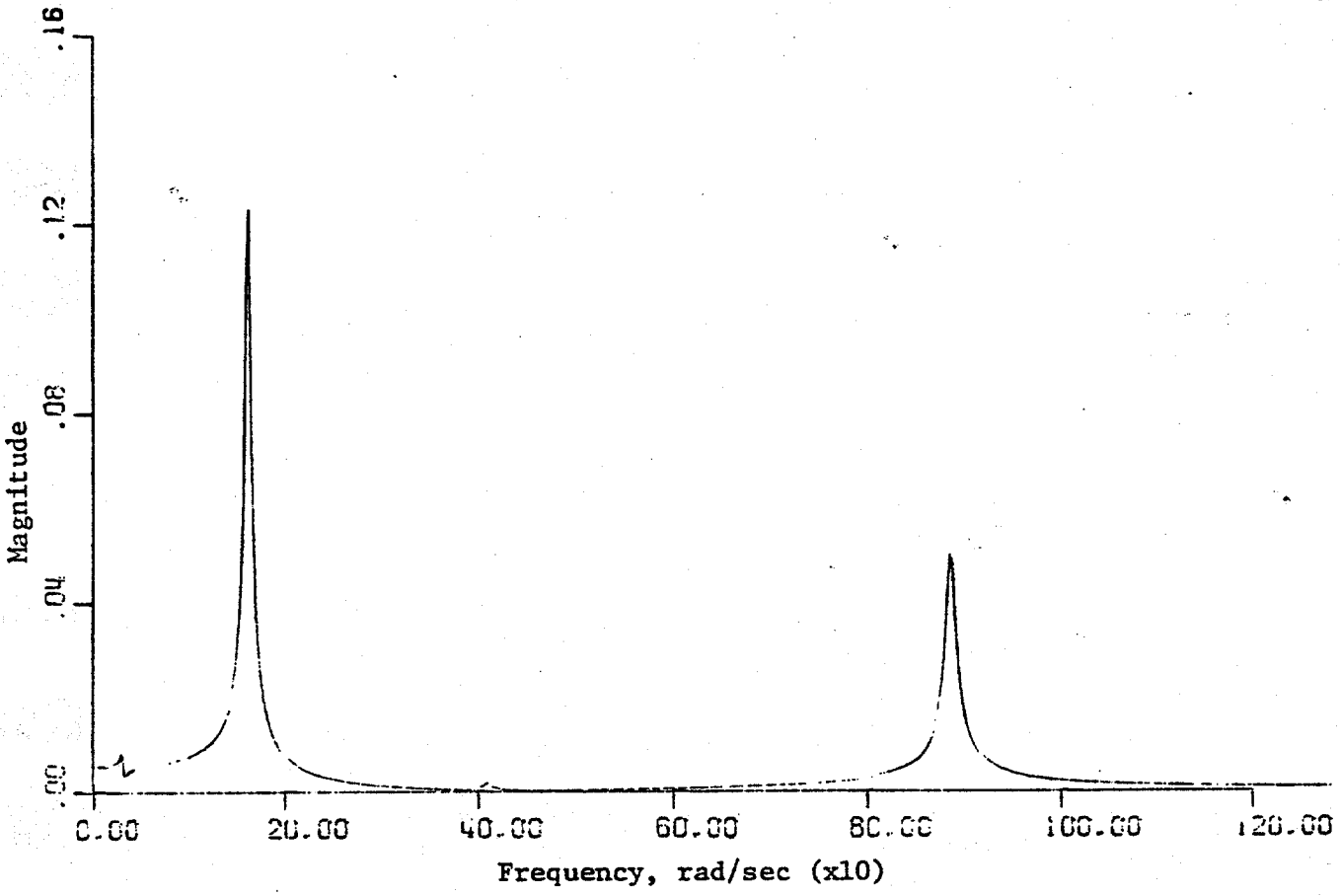

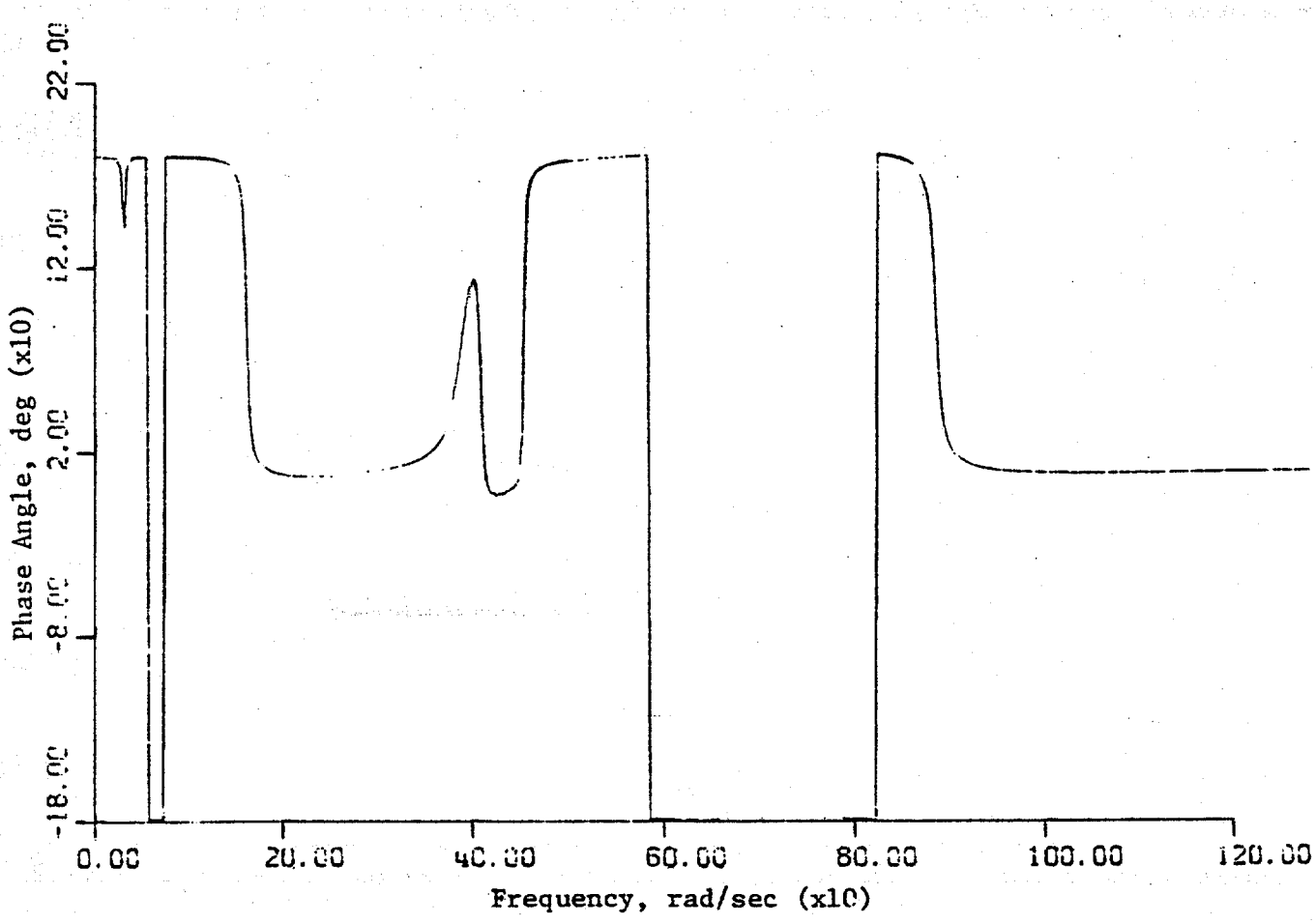

Fig. 4 Fitted Frequency Response, Magnitude and Phase Angle, with New Algorithm

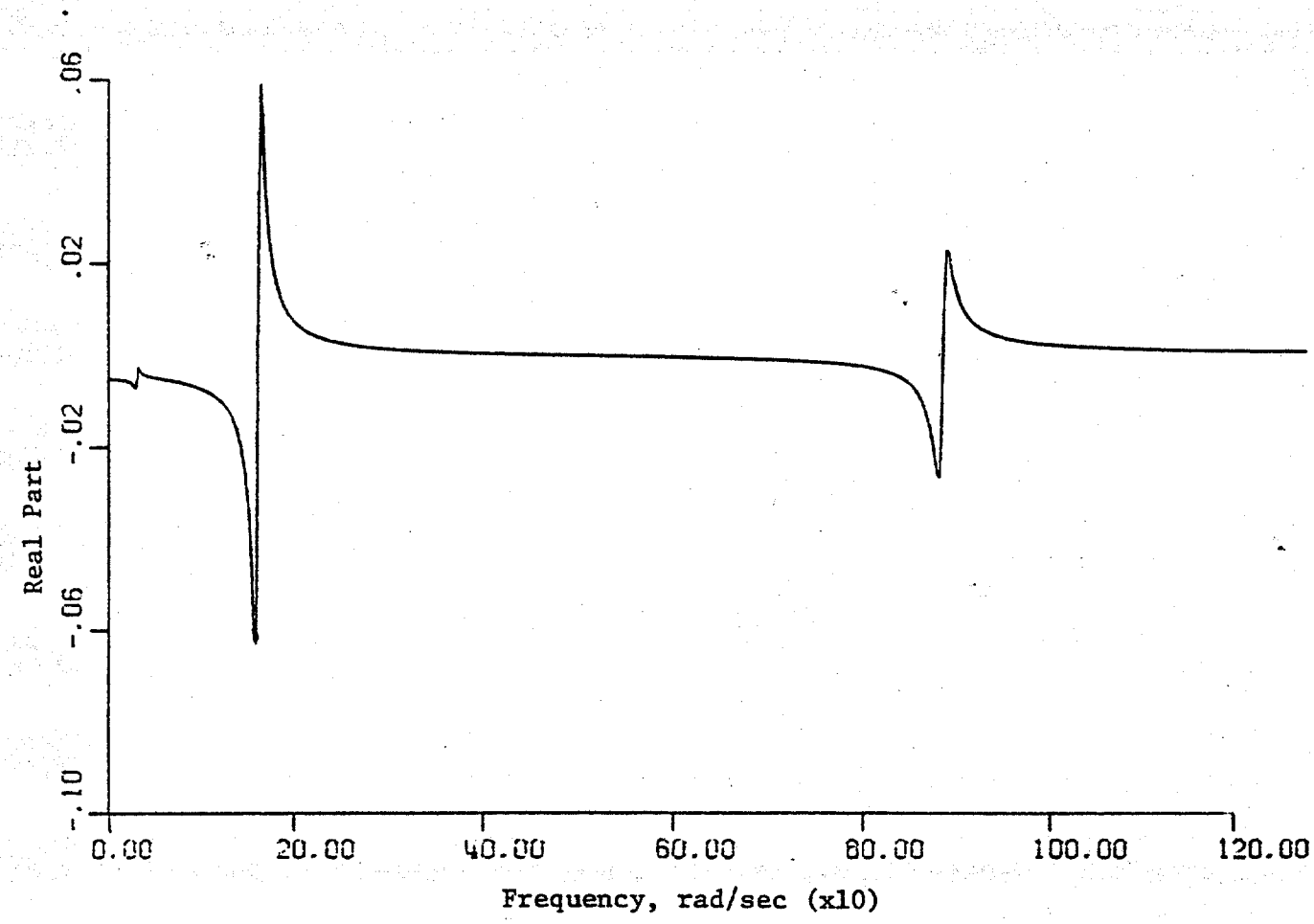

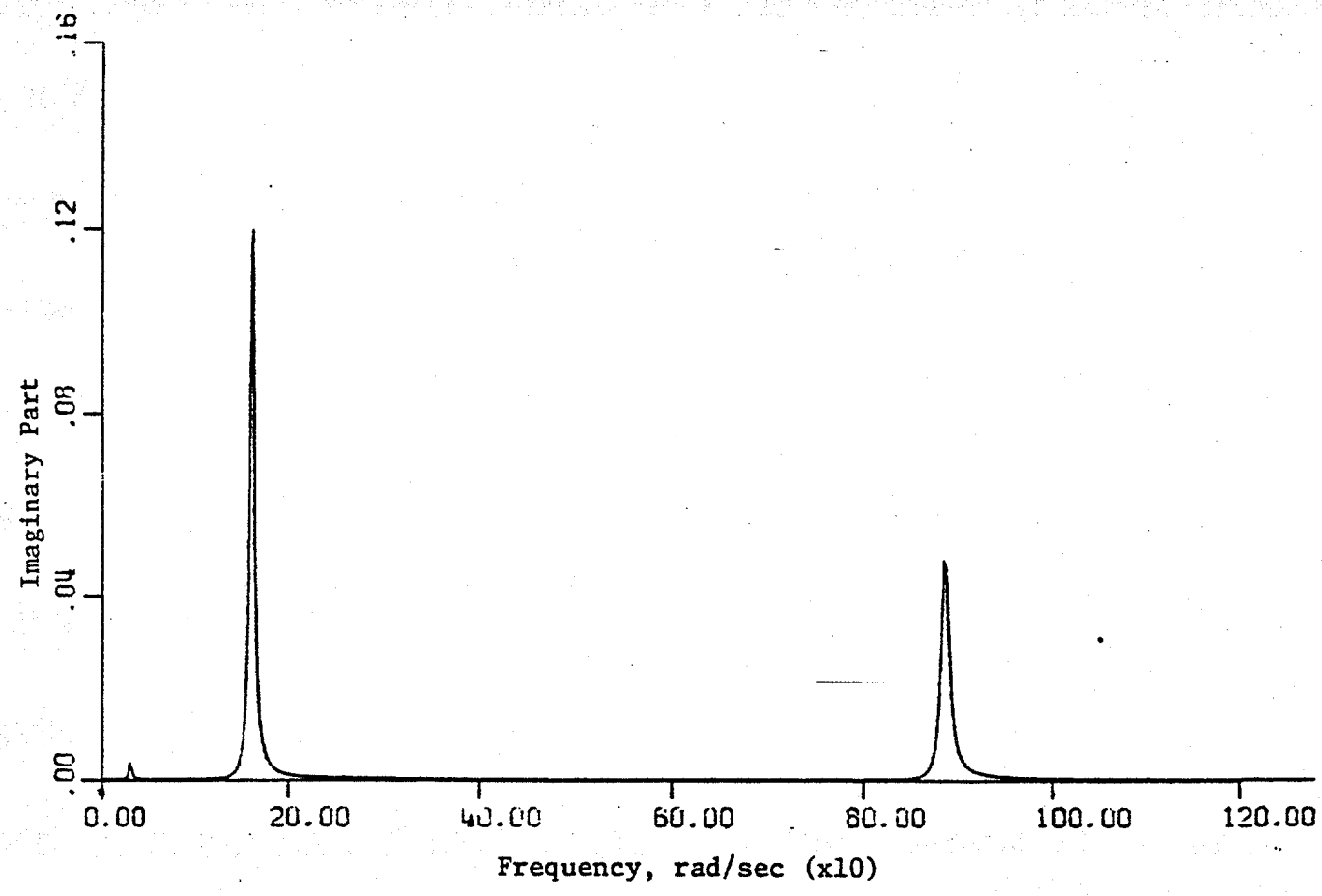

Fig. 5 Fitted Frequency Response, Real and Imaginary, with Sanathanan and Koerner Algorithm

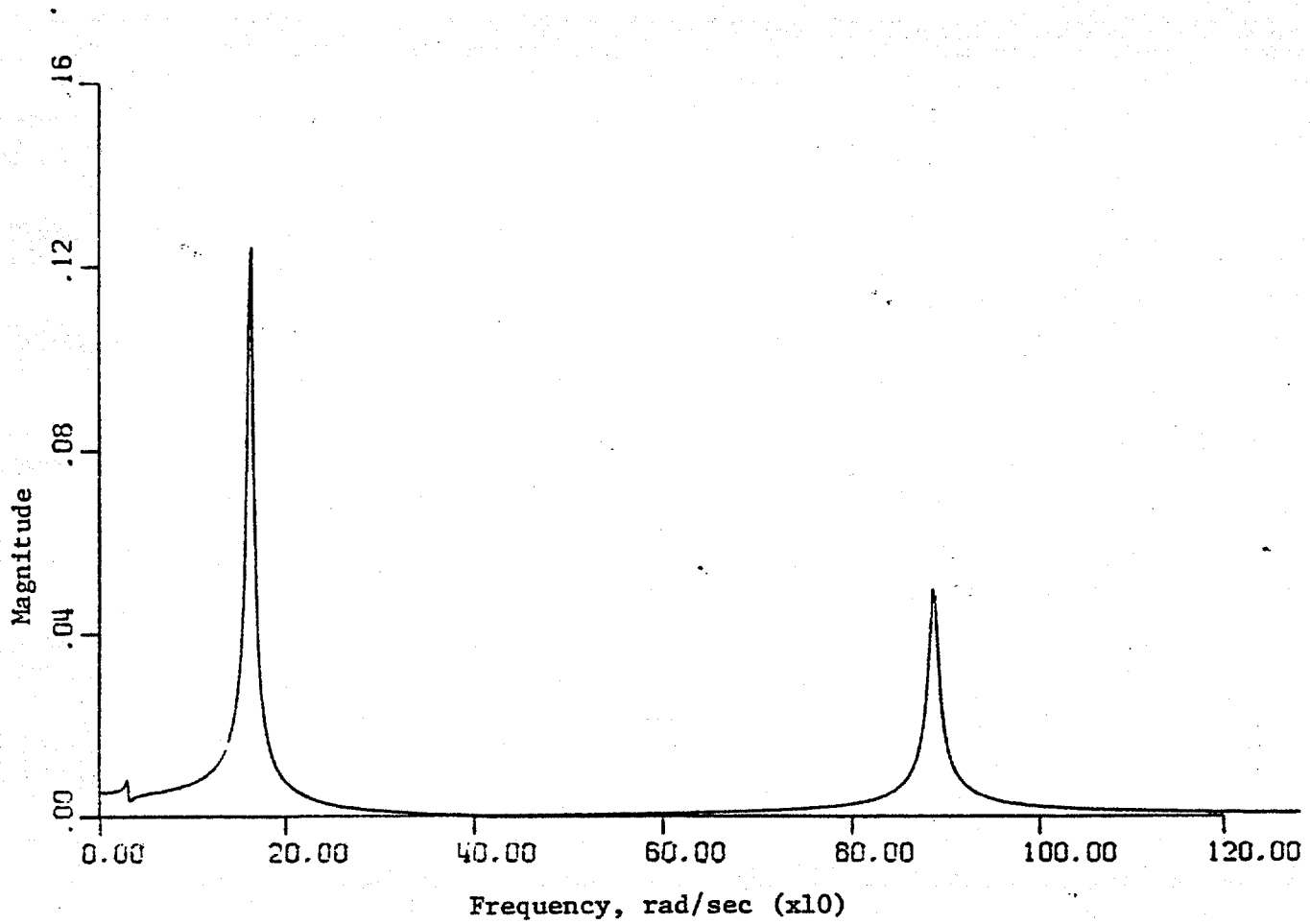

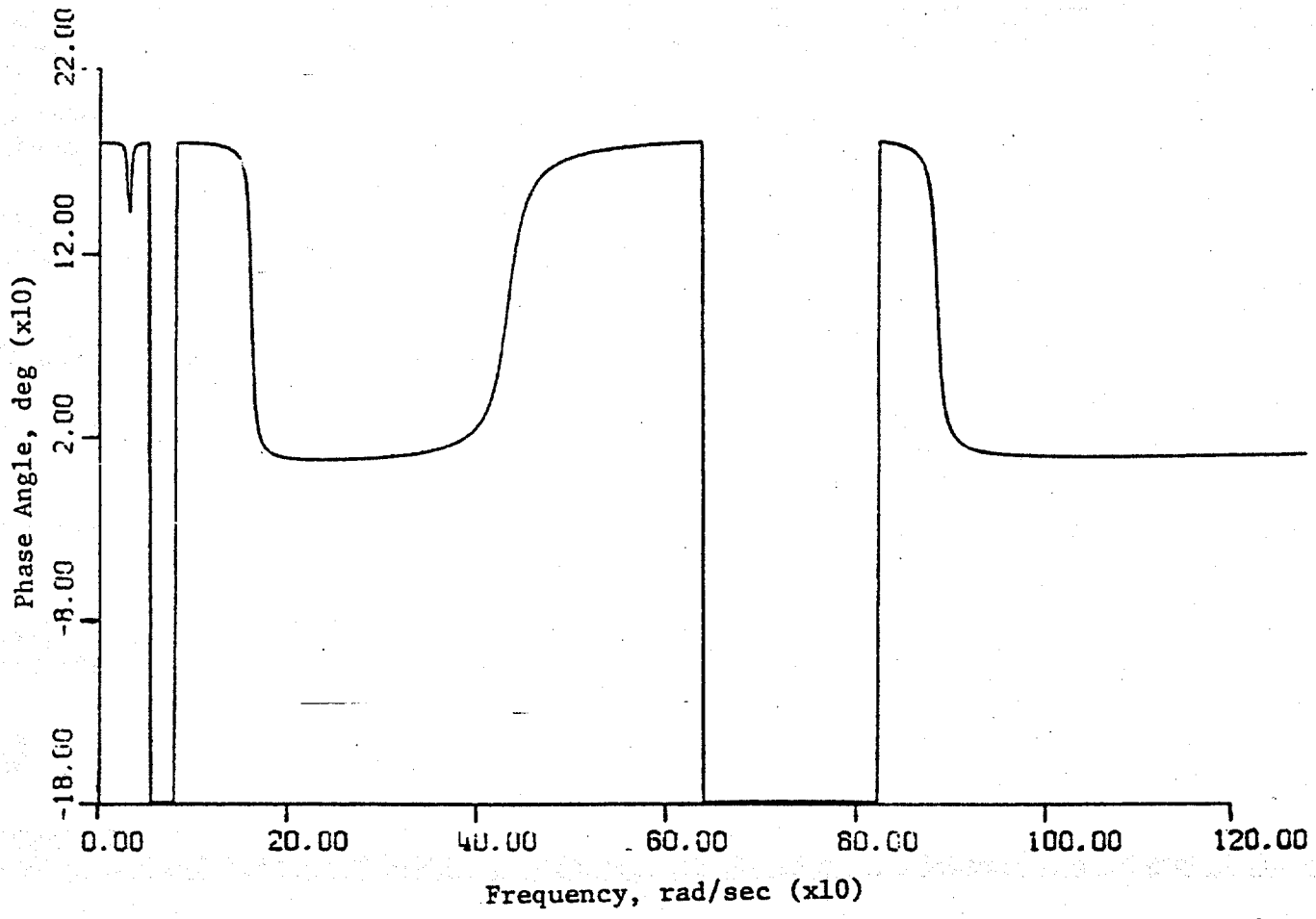

Fig. 6 Fitted Frequency Response, Magnitude and Phase Angle, with Sanathanan and Koerner Algorithm

REFERENCES

1. Andronikou, A. M., and Bekey, G. A., "Identifiably of Hysteretic Systems," Proc. of the 18th IEEE Conf. on Decision and Control, Dec. 1979, pp. 1072-1073.

2. Bekey, G. A., "System Identification, an Introduction and a Survey," Simulation, Oct. 1970, pp. 151-166.

3. Eshleman, R. L., "System Modeling," The Shock and Vibration Digest, Vol. 4(5), May 1972, p. 1.

4. Gersh, W., and Foutch, D. A., "Least-Squares Estimates of Structural System Parameters Using Convariance Function Data," IEEE Trans. Automatic Control, AC-19, 1974, pp. 898-903.

5. Hart, G. C., and Yao, J. T. P., "System Identification in Structural Dynamics, Dynamic Response of Structures: Instrumentation, Testing Methods and System Identification, ASCE/EMD Technical Conference, UCLA, March 1976.

6. Ibanex, P., "Review of Analytical and Experimental Techniques for Improving Structural Dynamic Models," Welding Research Council Bulletin, No. 249, June 1979.

7. McNiven, H. D., and Kaya, I., "Investigation of the Elastic Characteristics of a Three Story Steel Frame Using System Identification," U.C. Merkeley Report, No. EERC 78-24, Nov. 1978.

8. Marmarelis, W. Z., Masri, S. F., Udwadia, F. E., Caughey, T. K. and Jeong, J. D., "Analytical and Experimental Studies of the Modeling of a Class of Nonlinear Systems," Nuclear Engineering and Design, Vol. 55, 1979, pp. 59-68.

9. Masri, S. F., and Anderson, J. C., "Identification/Modeling of Nonlinear Multidegree Systems," Vol. 3, Analytical and Experimental Studies of Nonlinear System Modeling - A Progress Report AT (49-24-0262), U.S. Nuclear Regulatory Commission, Apr. 1980.

10. Masri, S. F., and Caughey, T. K., "A Nonparametric Identification Technique for Nonlinear Dynamic Problems," Journal of Applied Mechanics, Vol. 46, No. 2, June 1979, pp. 433-447.

11. Udwadia, F. E., and Marmarelis, P. Z., "The Identification of Building Systems - I. The Linear Case; II. The Nonlinear Case," Bull. of the Seism. Soc. of Amer., Vol. 66, No. 1, Feb. 1976, pp. 153-171.

12. M. Richardson, R. Potter, "Identification of the Mosfl Properties of an Elastic Structure from Measured Transfer Function Data," 20th I.S.A., Albuquerque, N.M., May 1974.

13. R. Potter, M. Richardson, "Mass, Stiffness and Damping Matrices from Measured Modal Parameters," I.S.A. Conference and Exhibit, N.Y., N.Y., Oct. 1974.

14. R. Potter, "A General Theory of Modal Analysis for Linear Systems," Hewlett-Packard Co., 1975.

15. W. G. Flannelly, J. H. McGarrey, A. Berman, "A Theory of Identification of the Parameters in the Equations of Motion of a Structure Through Dynamic Testing," U. of Technology, Loughborough, England, March 1970.

16. A. L. Klosterman, "On the Experimental Determination and Use of Modal Representations of Dynamic Characteristics, Ph.D. Thesis, U. of Cincinnati, 1971.

17. S. R. Ibrahim, E. C., Milulcik, "A Method for the Direct Identification of Vibration Parameters from the Free Response," Shock and Vibration Bulletin, Bulletin, 47, Part 4, Sept. 1977.

18. Volterra, V., Theory of Functionals and of Integral and Integro-Differential Equations, Dover, New York, M.I.T. Press, Cambridge, MA, 1959.

19. Wiener, N., Nonlinear Problems in Random Theory, M.I.T. Press, Cambridge, MA, 1958.

20. Lee, Y. W., and Schetzen, M., "Measurement of the Wiener Kernels of a Non-linear System by Cross Correlation," International Journal of Control, Vol. 2, 1965, pp. 237-254.

21. Simonian, S. S., "System Identification of Wind Forces in Structural Dynamics," Ph.D. Thesis, University of California, Los Angeles, Aug. 1978.

22. Cole, H.A., "Method and Apparatus for Measuring the Damping Characteristics of a Structure," United States Patent No. 3,620,069, 1971.

23. Cole, H. A., "On-Line Failure Detection and Damping Measurement of Aerospace Structures by the Random Decrement Signatures," NASA CR-2205, 1973.

24. Caldwell, D. W., "The Measurement of Damping and the Detection of Damage in Linear and Nonlinear Systems by the Random Decrement Technique," Ph.D. Thesis, University of Maryland, 1978.

25. Caldwell, D. W., "The Measurement of Damping and the Detection of Damage in Structures by the Random Decrement Technique," M.S. Thesis, University of Maryland, 1975.

26. Yang, J.C.S., Caldwell, D.W., "Measurement of Damping and the Detection of Damages in Structures by the Random Decrement Technique," 46th Shock and Vibration Bulletin, 1976, pp. 129-136.

27. Kummer, E., "The Detection of Fatigue Cracks in Structural Members by the Random Decrement Technique," M.S. Thesis, University of Maryland, 1979.

28. Yang, J.C.S., Aggour, M.S., Dagalakis, M., Miller, F., "Damping of an Offshore Platform Model by the Random Decrement Method," Proceedings of the Second ASCE/EMD Specialty Conference, Atlanta, Ga., pp. 819-832, 1981.

29. E.C. Levy, "Complex-Curve Fitting", IRE Trans. on Automatic Control, Vol. AC-4, pp. 37-44, May 1959.

30. C.K. Sanathanan and J. Koerner, "Transfer Function Synthesis as a Ratio of Two Complex Polynominals", IEEE Trans. on Automatic Control. Vol. AC-8, pp. 56-58, January 1963.

31. P.J. Lawrence and G.J. Rogers, "Sequential Transfer-function Synthesis from Measured Data", Proc. IEE, Vol. 126, No. 1, pp. 104-106, January 1979.

32. M.T. Jong and K.S. Shanmugam, "Determination of a Transfer Function from Amplitude Frequency Response Date", Int. J. Control, Vol, 25, No. 6, pp. 941-948, 1977.